1-1-1989

Neutron emmision-time distributions of methane moderators at the Argonne National Laboratory Intense Pulsed Neutron Source

Russell Lee Bywater
Iowa State University

Neutron emission-time distributions of methane moderators at the Argonne National Laboratory Intense Pulsed Neutron Source

by

Russell Lee Bywater, Jr.

A Thesis Submitted to the
Graduate Faculty in Partial Fulfillment of the
Requirements for the Degree of
MASTER OF SCIENCE

Major: Nuclear Engineering

Iowa State University
Ames, Iowa
1989

TABLE OF CONTENTS

LIST OF TABLES

LIST OF FIGURES

ABSTRACT

Slow neutrons are used by researchers in a variety of fields to study the structure of condensed matter. Neutron sources produce fast neutrons, which must be slowed down by moderators to energies of interest for slow-neutron spectroscopy. Time-of-flight spectroscopy techniques are used at pulsed neutron sources to sort neutrons according to wavelength. Assessment of the resolution of pulsed-source time-of-flight instruments and the analysis of data require knowledge of the emission-time distributions (pulse shapes) of neutrons emerging from the pulsed-source moderators. Measurements provide data of the pulsed-source moderator pulse shapes at discrete wavelengths. Mathematical functions are needed to provide good fits to the data and to accurately describe the pulse shapes for the entire range of wavelengths the moderator is used.

Measurements have been made of the pulse shapes as functions of energy for neutrons emerging from two liquid-methane and one solid-methane moderators at the Argonne National Laboratory Intense Pulsed Neutron Source. A time-focused germanium-crystal spectrometer arrangement was used in the measurements to decouple time resolution of a neutron pulse from spatial and angular resolution. Measurements of the liquid-methane F moderator covered the energy range $2.5 < E < 650$ meV. Measurements of the liquid-methane H moderator and

the solid-methane C moderator covered the energy range $2.5 < E < 1000$ meV.

Curve fitting techniques using the method of least squares were used to fit functions to the liquid-methane moderator data. The first function used in the curve fitting process was the Ikeda-Carpenter (IC) function. This function contains a "slowing-down" term, representing neutrons emerging from a moderator in the process of slowing down before thermalization, and a "storage" term, representing neutrons emerging from a moderator after thermalization. The IC function contains four wavelength-dependent parameters. The analysis of pulse shapes with this function, while maintaining all four parameters as free parameters for each energy, revealed substantial systematic deviations between the data and the best fitted function.

A form of the IC function with a generalization of the slowing-down term was then used to analyze the data. The generalized IC function contains five wavelength-dependent parameters. The analysis of pulse shapes with the generalized IC function, while maintaining all five parameters as free parameters for each energy, produced excellent fits. The observed wavelength-dependence of the parameters, however, was not as expected.

Postulated expressions for the wavelength-dependence of the parameters were used as constraints and pulse shapes were fit again with the generalized IC function. This procedure produced poorer fits. Constraints were imposed to eliminate two parameters from the fitting process. The fitting of pulse shapes was continued with only three free parameters for each energy. This resulted in good fits but the wavelength-dependence of the three free parameters was still not well behaved.

1 INTRODUCTION

After the discovery of the neutron by Chadwick in 1932, researchers were quick to realize this neutral constituent of atomic nuclei could have widespread application in scientific and engineering research. This realization has manifested itself in the rapid development of neutron sources over the years from the radioactive decay reactions, such as the (α,n) reaction in beryllium, to large scale fission reactors and accelerator-based sources of today. These sources are used by researchers in a wide range of disciplines including biology, chemistry, solid-state physics, and material science. The members of this diverse group of neutron users exploit the physical characteristics of neutrons and slow neutron spectroscopy techniques as excellent probes of the structure of matter [1]. The Intense Pulsed Neutron Source (IPNS) at Argonne National Laboratory is the world's first major pulsed spallation neutron facility dedicated to this work.

The IPNS utilizes moderators to provide researchers with the low energy neutrons required in their experiments. Neutron energies are determined by time-of-flight measurements. Knowledge of the emission-time distributions (pulse shapes) of neutrons emerging from the moderators as a function of neutron energy is essential information in the analysis of experimental data. This thesis describes measurements of these pulse shapes and attempts to fit these data with mathematical func-

tions. The remainder of this chapter provides introductory information on neutron sources, uses of neutrons, and the IPNS.

1.1 Neutron Sources

The neutron sources of primary use in condensed matter research may be categorized into two groups: (a) steady-state sources and (b) pulsed sources. Fission reactors comprise the first group with the high flux reactor at the Institut Laue Langevin, Grenoble, France being a prime example. The second group includes accelerator-based sources and pulsed reactors. Accelerator-based sources utilize an accelerator to bombard certain target materials with charged particles to produce neutrons. A variety of neutron producing reactions are possible depending upon the type of accelerator and target material used. The IPNS is an example of a source of this type, utilizing high-energy protons to bombard a target of uranium. IPNS will be more thoroughly described in section 1.3.

There has been considerable discussion on the comparison of advantages and disadvantages in the use of steady state or pulsed neutron sources [1], [2]. Steady-state reactor sources were the first to be developed and there is a correspondingly greater amount of experience in their use. They have limitations however, in that they produce more heat, which must be removed, per neutron produced, and neutron beams from a reactor are limited to a narrow energy band corresponding to the operating temperature of the reactor moderator. A large fraction of neutrons produced in a reactor source is wasted in neutron scattering experiments because of the monochromators or choppers that are used select neutrons of discrete wavelengths and discard others. In pulsed sources, time-of-flight spectroscopy conveniently sorts

a beam of neutrons according to wavelength.

Neutrons produced at either type of source may be categorized into three general groups: fast neutrons which are those neutrons recently produced in the fuel of a reactor or target of a pulsed source and which may have energies of several MeV; thermal neutrons which are those that have come into thermal equilibrium with the moderator of a neutron source, and have an average energy which is about equal to the mean energy of the surrounding material; finally, epithermal neutrons are those whose energy is above thermal (approximately greater than 0.1 eV) but not as high as fast neutrons. Regardless of which type of neutron source is under discussion, neutrons are produced with energies greater than 1 MeV [1], [3]. In order to be of use for condensed matter research using spectroscopy techniques, the neutrons must be slowed down to energies less than about 10 eV [1]. The neutron slowing down process is called moderation or thermalization and will be discussed in a later section. In pulsed neutron sources, the neutron moderation process imposes important constraints which must be quantified in order to obtain useful results from an experiment. Another benefit of pulsed sources is that the moderated neutron spectrum is especially rich in epithermal neutrons [1]. This avoids the limitation inherent in research reactors of having a narrow band of neutron energies available due to the temperature of the reactor thermal spectrum. Pulsed source moderators extend the range of neutron scattering experiments considerably [2].

Pulsed sources of neutrons utilize moderators placed close to the neutron producing target. Fast neutrons enter a moderator in a narrow time pulse governed by the time the beam is on the target. The thermalization process results in slow neutrons emerging from the moderator over a much broader time interval than the

fast-neutron pulse in view of the time required between energy-reducing collisions. The emission-time distribution or pulse shape of neutrons emerging from the moderator is a function of the physical properties of the moderator and the neutron energy.

1.2 Slow Neutrons as a Tool in Scientific Research

Neutrons are the neutral constituents of atomic nuclei. They have nearly the same mass as the proton but have no electric charge. Since they are uncharged particles, neutrons are able to penetrate into the volume of a sample without experiencing forces due to the electric field associated with protons or electrons. In addition to absorption reactions, neutrons interact weakly with materials in two ways. First, they may undergo nuclear scattering which is the result of the short-range interaction associated with the nuclear interaction. Second, neutrons carry a magnetic moment and may be scattered by magnetic interaction with materials.

Neutrons have associated de Broglie wavelengths and may exhibit wave behavior as well. Energy and wavelength units are equivalent in describing neutrons. Research workers in different areas use different energy-related variables as a matter of convenience. For instance, diffractionists talk in terms of wavelength, spectroscopists and engineers in terms of energy, theorists in terms of lethargy, etc. [4]. Energy and wavelength variables will be used in this thesis according to context and convenience. The de Broglie wavelengths of slow neutrons are of the order of the interatomic spacings in condensed matter and so are well suited for study of their structure and dynamical behavior [5].

Two areas of slow neutron research dominate the use of the Intense Pulsed Neu-

tron Source. They are neutron diffraction and inelastic neutron scattering. Windsor [2] discusses these areas of research and experimental techniques. In neutron diffraction measurements at IPNS, neutrons are allowed to scatter from a sample into a detector. The neutrons are sorted according to wavelength by measuring the time it takes them to travel from the source to the detector. This is called time-of-flight spectroscopy. The measured quantity of interest in a neutron diffraction measurement is the intensity of detected neutrons as a function of a quantity $d = \lambda/(2\sin\theta)$. In the study of crystalline solids, d is the spacing of planes in the crystal lattice. The quantity λ is the neutron wavelength and θ is one-half the neutron scattering angle. Time-of-flight sorting allows λ to be varied while θ is constant so that intensity as a function of d may be determined. Measurements of this type allow researchers to determine the atomic arrangements of atoms in condensed matter.

In inelastic scattering measurements at IPNS, neutrons pass through a wavelength selecting device called a chopper to produce a beam of neutrons of one energy. These are allowed to scatter from a sample into a detector. The measured quantity of interest in an inelastic scattering measurement is the intensity of detected neutrons as a function of energy and scattering angle. These measurements allow researchers to determine the frequencies of atomic motions in a sample, which are directly related to the binding forces between atoms.

Neutron scattering measurements provide excellent tools for the study of matter. To be successful these instruments require a reliable, high-intensity source of neutrons; the Intense Pulsed Neutron Source helps to fulfill this need.

1.3 The Intense Pulsed Neutron Source

The first section of this thesis defined the two general categories of neutron sources: steady state sources and pulsed sources. In the pulsed-source category, several neutron production mechanisms are available including pulsed research reactors, electron bremsstrahlung photoneutron sources, spallation neutron sources, and laser-imploded pellet fusion sources. The Intense Pulsed Neutron Source is a spallation source. This section describes the spallation neutron production process and presents a basic operational description of IPNS.

1.3.1 Spallation neutron production at the IPNS

Spallation is a complicated multicollision process that occurs when high-energy charged particles bombard a target of some high-mass-number material [1]. At IPNS, protons accelerated to an energy of 450 MeV are used to bombard a target of uranium. At the time of data collection for the measurements reported in this thesis, a depleted uranium target was in use. In October 1988 a "booster" target of 77.5 % enriched ^{235}U was installed to increase the neutron yield by taking advantage of fission reactions.

When the energetic protons impinge upon the target they first interact with the most loosely bound target nucleons resulting in a cascade of neutrons and protons which then may collide with other target nuclei and thus produce additional neutrons. Neutrons produced in this manner have energies up to that of the incident protons and have a direction of emission strongly peaked in the direction of the proton beam. As a result of the cascade, target nuclei are left in an excited state and return to ground state through the evaporation of additional neutrons.

Evaporation neutrons are produced isotropically and have lower energies of perhaps a few MeV. Fission reactions are important in targets containing fissionable or fissile material as neutrons result from these reactions as well.

The neutron spectrum of a spallation target is dominated by the lower energy fission and evaporation neutrons with only a few percent of the spectrum composed of the high energy cascade neutrons. It is these cascade neutrons that dominate shielding requirements, however, and thicker shields than are used in reactors are required [1].

The amount of heat deposited in a spallation target depends on many factors. The incident particle energy determines the energy spectrum of spallation products. The target size and geometry influence how much energy leaves the target as particles escape the target and deposit their kinetic energy elsewhere. Finally, heat production depends on the quantity of fissionable material in the target, because each fission event deposits about 180 MeV locally in the target. It is very important that provisions be made for an adequate cooling system to remove the heat from a spallation target. The IPNS depleted uranium target produced a thermal power of about 10 kW. The IPNS booster target has an estimated thermal power of about 83 kW [6]. A significant factor to be considered in target and cooling system design is the heat production due to fission events.

The production of delayed neutrons must be accounted for in targets containing fissionable material. It is known when a material fissions, a certain fraction of the neutrons produced do not appear at the instant of fission. Instead, they appear after some time delay due to the fission products undergoing beta decay and subsequent neutron emission. The fraction of neutrons produced in this way is called the

delayed neutron fraction and represent approximately 0.02 neutrons/fission and 0.05 neutrons/fission for ^{235}U and ^{238}U, respectively [3]. These delayed neutrons are responsible for a time-independent background source. Although these neutrons constitute a small fraction of the total number of neutrons produced, they may cause unacceptable background levels in some experiments. Carpenter [7] has measured the effective delayed neutron fraction of the IPNS depleted uranium target to be 0.0053. The delayed neutron fraction of the enriched uranium booster target is estimated to be 0.03 [6] (larger than the fraction for each fission because of subcritical multiplication effects).

With the above discussion on some of the extra things that must be accounted for with an enriched uranium target, the reader may wonder why such a target is desirable. The answer is that ^{235}U has a much higher fission cross section than ^{238}U and unlike ^{238}U, which has a fission threshold at about 1 MeV, ^{235}U may be caused to fission by neutrons of any energy. This increases the neutron yield of the target considerably and, in the case of the IPNS booster target, has raised the neutron yield by a factor of about 2.5 [8].

1.3.2 Operational arrangement of the IPNS

The following is a description of the IPNS facility. The arrangement of the accelerator system is shown in Figure 1.1. The process of neutron production begins with the insertion of H^- ions from an ion source into a Cockcroft-Walton preaccelerator where they are accelerated to 750 keV. The ions are then inserted into a 35-m Alvarez linac and accelerated to 50 MeV.

The pulse ions are magnetically steered to the 14-m diameter rapid cycling

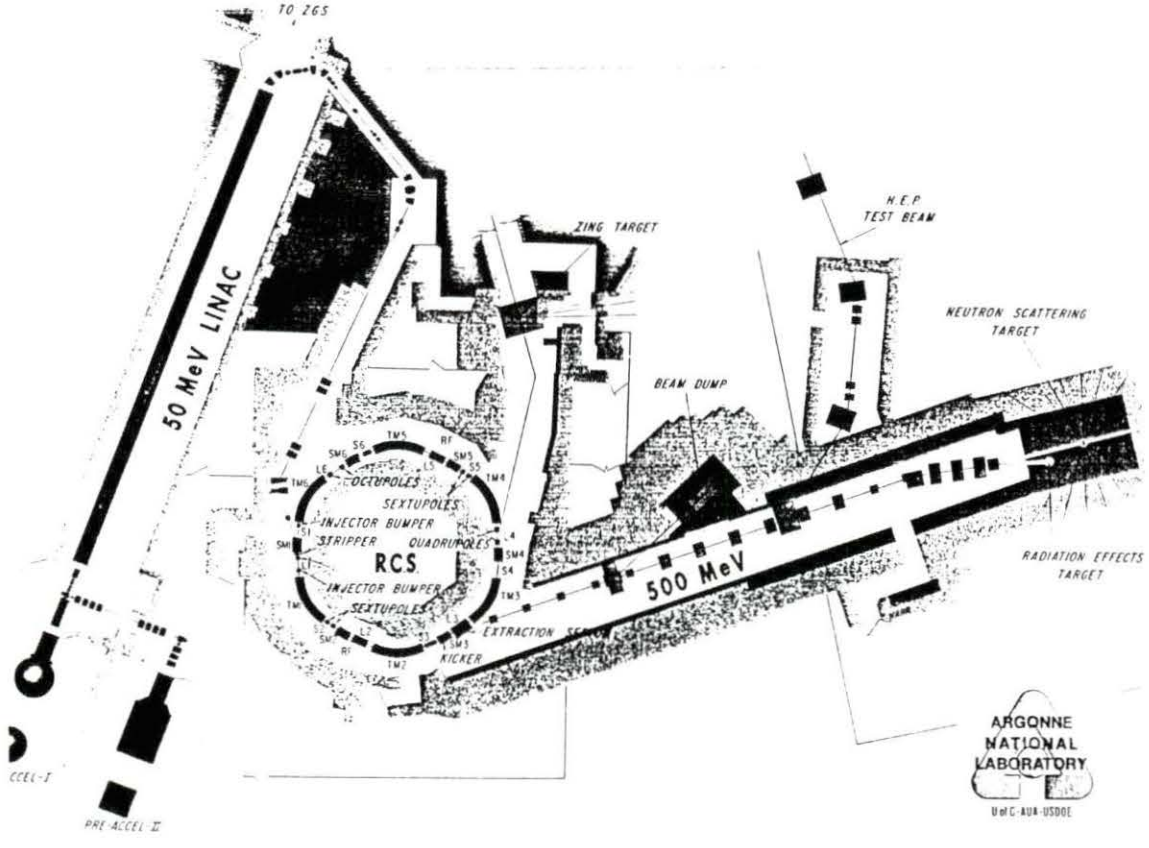

Figure 1.1: Arrangement of the IPNS accelerator system

synchrotron (RCS). At injection, the H^- ions pass through a thin carbon foil which strips two electrons from each ion leaving an H^+ ion, or proton. The protons are accelerated to 450 MeV and released in 80 ns pulses at 30 Hz to be delivered to the neutron producing target. One measure of the performance of the IPNS accelerator system is the "proton beam current" on target. During normal operation, the accelerator system provides ≈ 13 μA of proton current to the target.

The depleted uranium target consisted of eight 25-mm thick disks clad with a 0.5-mm layer of Zircaloy-2. The disks were contained in a stainless steel target housing with provision made for light water cooling channels between the disks. (The enriched uranium booster target currently in use has thinner disks at the front of the target to provide additional surface area for its greater cooling requirements.)

During the time when measurements used for this thesis were obtained, the fast neutrons produced in the depleted uranium target were slowed down by two liquid methane moderators at a temperature of about 100 K and one grooved solid methane moderator at about 15 K. (After the booster target was installed, the solid methane moderator was changed to liquid hydrogen.) The moderators and target assembly are embedded in an inner graphite reflector, and surrounded by an outer beryllium reflector. The reflectors return neutrons that have leaked out of the moderators before thermalization and also may scatter neutrons back into the target for the possibility of causing another neutron producing reaction. Decoupling material surrounding the moderators prevents long-lived slow neutrons from the reflector from returning to the moderators. The target-moderator-reflector assembly is surrounded by steel and concrete biological shields.

Twelve beam paths are oriented horizontally and face a selected view of a

Table 1.1: IPNS instruments

Diffractometers		
SEPD	Special Environment Powder Diffractometer	F5
GPPD	General Purpose Powder Diffractometer	F2
SCD	Single Crystal Diffractometer	F6
SAD, SAD II	Small Angle Scattering Diffractometers	C1,C3
GLAD	Glass, Liquid, and Amorphous Material Diffract.	H1
Spectrometers		
LRMECS	Low-Resolution Medium-Energy Chopper Spect.	F4
HRMECS	High-Resolution Medium-Energy Chopper Spect.	H3
eVS	Electron-volt Spectrometer	F3
QENS	Quasielastic Neutron Spectrometer	H2
PHOENIX	High Resolution Chopper Spectrometer	F1
Reflectometers		
POSY, POSY II	Polarized and Unpolarized Neutron Reflect.	C2 (both)

moderator. Figure 1.2 shows the IPNS experimental hall. Each beam path has a letter and number corresponding to it and an acronym for the neutron scattering instrument located within it. The beam path letter designation indicates which moderator a particular beam path is viewing. Moderators 'F' and 'H' were liquid methane and moderator 'C' was solid methane. Table 1.1 identifies and categorizes the instruments. Diffractometers are used in neutron diffraction experiments, spectrometers are used in inelastic scattering experiments, and reflectometers are used in determining the magnitization of materials.

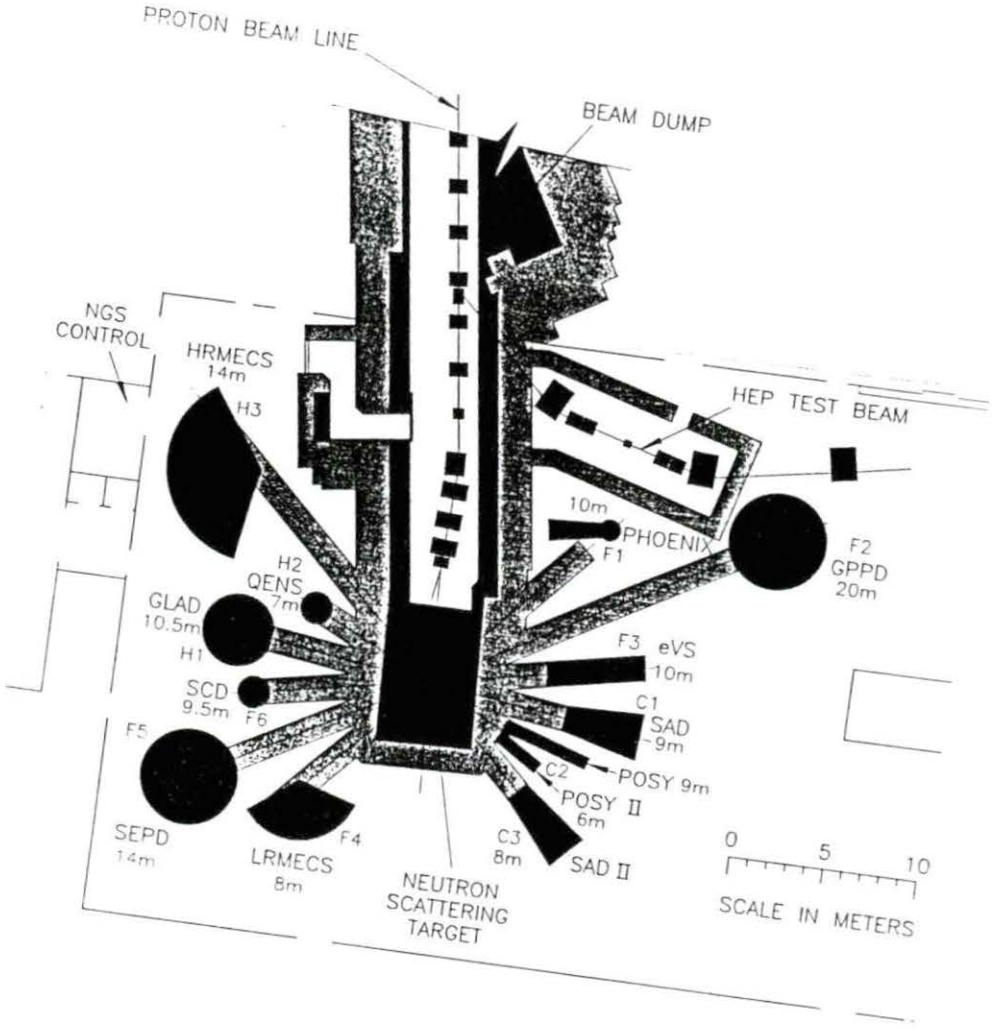

Figure 1.2: Arrangement of the IPNS experimental hall

2 BACKGROUND

This chapter presents background information on neutron moderation in pulsed sources, an explanation of why mathematical functions which describe the shape of neutron pulses from the moderators are necessary, and a brief history of their development. Since all new research builds on past work, knowledge of the theory of neutron moderation and the history of pulse shape fitting functions benefits moderator pulse shape analysis. Indeed, the final pulse shape fitting function used in this thesis, a generalization of the Ikeda-Carpenter Function, has evolved through the review of its predecessors and neutron slowing-down theory.

2.1 Neutron Moderation

In this section, a brief description of neutron moderation, with specific application to pulsed source moderators, will be presented. Neutron moderation and the thermalization of neutrons is an extensive subject and many works are devoted to it. A thorough exposition of the theory of thermalization with emphasis on mathematical models is provided by Williams [9]. Parks et al. [5] have produced a similar presentation of theory but they extend it to include discussion on applications of moderators and results of experimental work on moderators. Ferziger and Zweifel [10] have devoted a text to neutron moderation in reactors. In addition,

texts in reactor theory [11], [3], devote chapters to discussion of neutron moderation. Although nuclear reactors are quite different entities than pulsed neutron sources, the same processes of neutron slowing down occur in the moderators of both. Through their education in reactor theory, nuclear engineers are prepared to aid in the design and analysis of moderators at a pulsed neutron source.

Neutrons produced in the spallation and fission reactions in a pulsed neutron source are very energetic (as far as neutron scattering experimentalists are concerned), having an average energy greater than 1 MeV. In the moderators, these neutrons lose their energy by undergoing a series of elastic and inelastic collisions with the moderator nuclei. It is convenient in the discussion of neutron moderation to divide the energy spectrum of neutrons into two regions where separate methods of describing the neutron population are used.

The first region to be considered encompasses those neutron scattering events in which the energy of the incident neutron is greater than some cutoff energy E_{co}, defined by the temperature of the moderator. Above this energy the moderator nuclei may be assumed to act as free particles, unrestrained by any binding effects on a molecular scale. In addition, if the neutron energy is greater than E_{co}, the moderator nuclei may be assumed to be stationary before the collision. The density of neutrons in this energy region follows a $1/E$ dependence. This region is called the moderating, slowing-down, or epithermal region. Hence, the process of neutrons slowing down in this region is called moderation.

The second region to be considered in neutron slowing-down theory is that region characterized by neutron energies less than E_{co}, or simply the thermal region. Moderator nuclei can no longer be assumed to behave as free particles; their

chemical binding effects must be considered. These binding effects of moderator nuclei complicate the process of neutron scattering by allowing different types of scattering events to take place. Examples are excitations of vibrational, rotational, or translational modes of moderator molecules, or, if the moderator is crystalline, Bragg scattering in the crystal lattice.

Another important attribute of this lower region is that because of the thermal energy the moderator nuclei possess, they are in constant motion and may actually impart energy to a neutron, increasing the neutron energy. This "upscattering" phenomenon is analogous to what occurs to molecules in a gas at thermal equilibrium. The neutrons have reached an approximate state of thermal equilibrium with the nuclei of the moderator, and like a gas, acquire a Maxwell-Boltzmann distribution of energy. The most probable energy of the neutrons is given by $E = kT$ where k is Boltzmann's constant and T is the effective temperature of the moderator. Neutrons which have lost enough energy through scattering events to be in a state of thermal equilibrium with the moderator nuclei are said to have been "thermalized" and this region of the neutron spectrum is called the thermal region of the spectrum.

In the vicinity of the cutoff energy E_{co}, the neutron spectrum has some upscattering which helps define the spectrum shape as somewhat Maxwellian, yet, upscattering is not as important here as at lower energies. Likewise, the neutron spectrum has some similarity to the slowing-down spectrum of higher energy, but the effects in neutron scattering due to thermal motions and chemical binding are distorting the spectrum somewhat. This is called the transition or joining region and represents the subtle change of a slowing-down neutron distribution into a ther-

mal one. The joining region can be thought of as the "cutoff" of the epithermal spectrum, occurring at energy E_{co}. In practice $E_{co} \approx 5kT$ [11].

The neutron flux in a moderator may be expressed mathematically using the above concepts of neutron behavior in different energy regions. The neutron flux per unit energy at energy E in a moderator is given by

$$\phi(E) = \phi_{max} \frac{E}{(kT)^2} exp\left(-\frac{E}{kT}\right) + \phi_{epi} \frac{\Delta(E)}{E^{1-\alpha}}, \tag{2.1}$$

where ϕ_{max} and ϕ_{epi} are constants and α is the "leakage exponent" accounting for neutron leakage from finite moderators. The first term is the Maxwellian component of the spectrum, dominant at low energies, and the second term is the slowing-down component of the spectrum, and is dominant at higher energies. The dominance of one term over another is determined by the joining function $\Delta(E)$. Taylor, as cited in [12], has suggested as a functional form of the joining function

$$\Delta(E) = \left[1 + exp\left(\frac{A}{\sqrt{E-B}}\right)\right]^{-1}, \tag{2.2}$$

where A and B are empirical constants. The joining function maps energy to a dimensionless number between zero and one, tending to zero in the thermal region and one in the epithermal region. Figure 2.1 [13], [2] shows, on a wavelength scale ($\lambda \propto 1/\sqrt{E}$), the measured neutron spectrum of a room temperature polyethylene moderator. The solid curves indicate the fitted components of the spectrum using Equation (2.1).

The information on neutron moderation presented in this section forms the foundation for all other problems associated with the slowing down of neutrons. The next section will present the problem of describing the moderation of a pulse

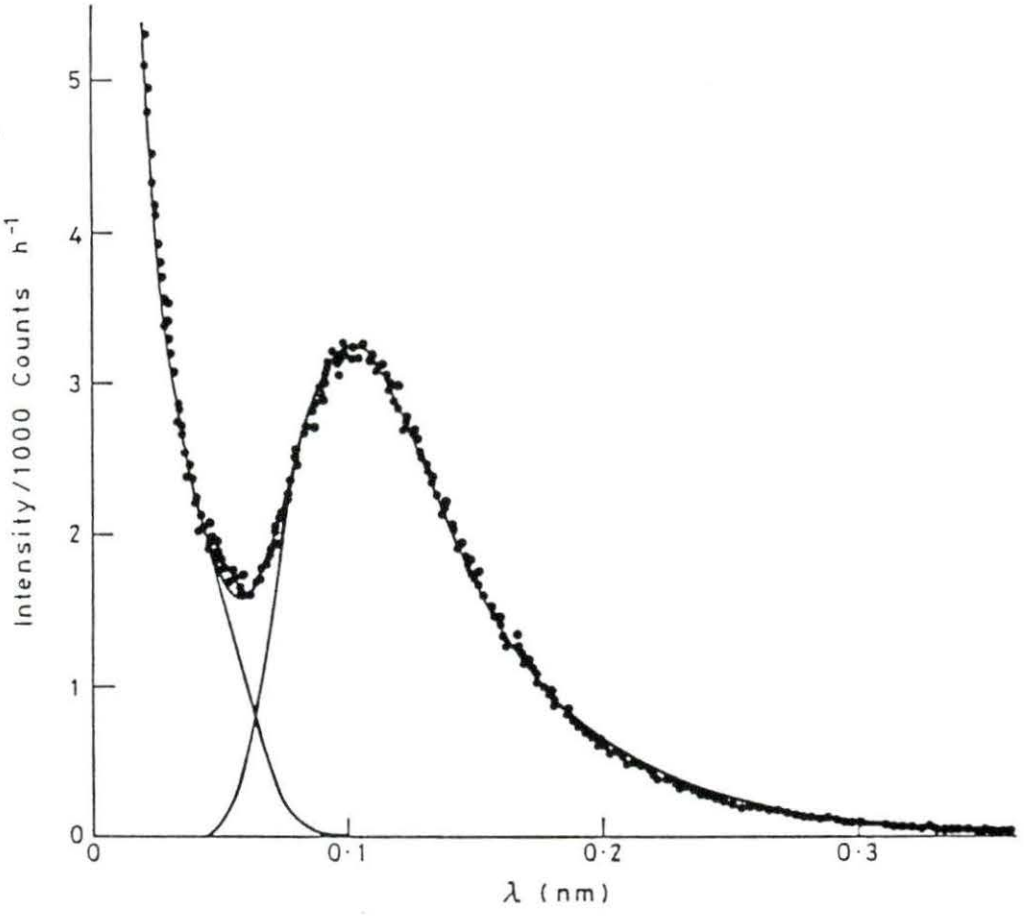

Figure 2.1: The neutron spectrum of a polyethylene slab moderator at room temperature

of neutrons and give a brief history on the development of fitting functions used to describe the shapes of pulses emerging from a pulsed source moderator.

2.2 Pulse Shape Fitting Functions

Fast neutrons are produced at IPNS in short ($\approx$ 100 ns) pulses at a frequency of 30 Hz. These fast neutrons enter the moderators and their energy is reduced through elastic and inelastic collisions with the moderator nuclei. The slowing down time, t_s [11], required for a neutron to become thermalized depends upon the moderator temperature and composition. A high flux of slow neutrons from the surface of the moderator, following the source pulse of fast neutrons, is desired in slow neutron research in a pulse as short as possible. It is noted that due to the kinematics of neutron scattering, neutrons can lose more of their energy in collisions with protons than with any other scattering material. For this reason dense hydrogenous materials such as liquid hydrogen, liquid or solid methane, water, or polyethylene are often used as moderators. Cooling a moderator to cryogenic temperatures has added benefits in neutron moderation for slow neutron work. The Maxwellian portion of the neutron spectrum is pushed to lower energies and the epithermal spectrum is extended to lower energies as well, producing a desirable increase in the number of long-wavelength neutrons and narrowing the pulse at intermediate energies. In addition, cooling a moderator increases its density and decreases the neutron path length between scattering events. This shortens the neutron slowing down time and the neutron pulse width [14].

In examining the behavior of a pulse of fast neutrons injected into a moderator, we again will divide the spectrum into separate components at the point where the

thermal and chemical binding effects of the moderator are not important ($E \approx 5kT$). In the high energy range, the neutron spectrum has the form of the Grueling-Goertzel approximation of neutrons slowing down in an infinite medium of free protons. The instantaneous neutron beam current per unit energy may be expressed as a function of neutron velocity and time after the initial pulse as [4]

$$I(v,t) = \frac{\xi\Sigma_s v}{2\Gamma(2/\gamma)} \left(\frac{\xi\Sigma_s vt}{\gamma}\right)^{2/\gamma} exp\left(-\frac{\xi\Sigma_s vt}{\gamma}\right), \tag{2.3}$$

where Σ_s is the macroscopic scattering cross section of the moderator, and v is the neutron velocity. For materials with large mass number A, $\xi \approx 2/A$ and $\gamma \approx 4/3A$. In monoatomic materials, ξ is the mean logarithmic energy change per collision and $2\xi\gamma$ is the mean-squared logarithmic energy change per collision. For dense hydrogenous moderators, $\xi \rightarrow 1, \gamma \rightarrow 1$, and the time distribution of the neutron slowing down distribution reduces to

$$I(v,t) = \frac{\Sigma_s v}{2}(\Sigma_s vt)^2 exp(-\Sigma_s vt). \tag{2.4}$$

Literally, Equation (2.3) is the time distribution of a pulse of neutrons slowing down in an infinite medium of protons (the "proton gas" model). In finite moderators, pulses are slightly narrower due to neutron leakage effects and neutron absorption.

When the neutron energy is on the order of the thermal energy of the moderator nuclei, there does not exist a simple description of the time- and energy-dependent neutron distribution. In nuclear reactor engineering, pulsed-neutron experiments are used in subcritical assemblies for determining the critical dimensions of the assembly, the thermal diffusion area, and the thermal diffusion time of the moderator [11], [3]. In these experiments, the thermal neutron flux is measured at some point in the assembly. At long times after the pulse, the neutron flux decreases

exponentially with a decay constant β. The decay constant is directly related to the geometric buckling, B_g^2, of the assembly, and if a series of measurements of β are made as a function of B_g^2, the critical reactor dimensions may be determined.

This is a rather simplified application of the theory of the thermalization of a pulse of neutrons. The actual thermalization process of the pulse is a complex eigenvalue problem which is described in detail by Williams [9]. Carpenter and Yelon [4] conclude their summary of William's discussion of this problem with some observations:

> (1) At long times, for low energies, and in moderators that are not too small, we can expect exponential decay of a pulse, whose decay is faster the smaller the moderator.
>
> (2) There are several exponentially decaying terms corresponding to spatial modes of different bucklings.
>
> (3) In moderators that are not too small, the energy distribution approaches a Maxwellian at long times.
>
> (4) We can expect exponentially decaying transients within a given spatial mode, which represent relaxation to the asymptotic energy distribution.

The thermalization problem is obviously quite complex and an analytical solution for the neutron emission-time distribution of a pulsed moderator would be extremely difficult to obtain. Measurements of these distributions have been made in order to provide data for fitting mathematical functions which would describe the distribution. Over the years there has been a trend away from functions that

were completely empirical and toward the development of functions that make an attempt to include some of the physics of the thermalization problem.

Figure 2.2 [4] shows schematically three functions that have been developed to describe the shapes of neutron pulses from moderators as a function of energy. Although the basic principles of neutron slowing-down theory are too complicated for direct use in the data analysis of neutron scattering experiments, the theory can provide insight in the development of fitting functions.

The function represented in Figure 2.2 (a) has been especially useful in the analysis of experimental data from powder diffractometers. The function was developed by Jorgensen, as cited in [15]. It is the sum of a rising exponential and a falling exponential, joined continuously at the zero of the time scale and has four wavelength-dependent parameters. This function combines effects of powder diffractometer geometry as well as the moderator pulse shape. Kropff, Granada, and Mayer [16] describe this function in detail and outline how they used it to fit the shapes of Bragg peaks of powder diffractometer spectra. The Jorgensen function works well for experiments using polyethylene moderators but is limited because it implies neutrons may emerge from the moderator before the source pulse and it does not fit the pulse shapes of methane moderators very well [4].

The function represented in Figure 2.2 (b) is of the same form as the previous function but it is an improvement. It does not have neutrons emerging before the source pulse and it provides a better description of the pulse shapes of methane moderators. It not only accounts for the moderator pulse shape but for instrument induced Gaussian-broadening as well. The function was developed by Carpenter, Taylor, and Robinson, as cited in [12] and is the convolution of a Gaussian with

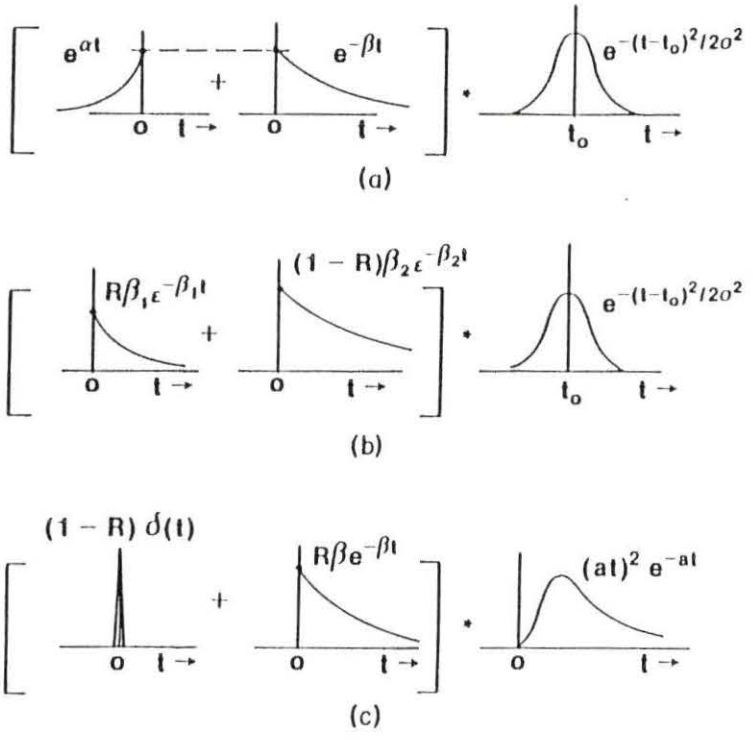

Figure 2.2: Schematic representations of several moderator pulse shape functions

two decaying exponentials. This function has five wavelength-dependent parameters, including one of the decay constants (β_2); the other decay constant (β_1) is wavelength-independent.

The function represented in Figure 2.2 (c) was developed by Ikeda and Carpenter [17]. The Ikeda-Carpenter (IC) function is intended to be a better physical description of moderator neutron pulse shapes. It does not account for instrumental effects like the two previous functions. The IC function is the convolution of a slowing-down function with the sum of a delta function and decaying exponential. This is the function first tried in the analysis of pulse shape data in this thesis. The function may be expressed in its time-distribution form with four wavelength-dependent parameters as

$$i(v,t) = \frac{a}{2}\left\{(1-R)(at)^2 e^{-at} + 2R\frac{a^2\beta}{(a-\beta)^3}\right.$$
$$\left.\times[e^{-\beta t} - e^{-at}(1+(a-\beta)t + \frac{1}{2}(a-\beta)^2 t^2)]\right\}, \qquad (2.5)$$

where $i(v,t)$ is the observed instantaneous beam current, $a = v\Sigma_s$, v is the neutron velocity, Σ_s is the moderator macroscopic cross section, R is the ratio of the area of the second term to the total area, t is the time after the source pulse, and β is the decay constant of the fundamental mode neutron distribution. The first term in the IC function is the $1/E$ slowing-down component, representing neutrons that have emerged from the moderator in the process of slowing down before thermalization. The second term is the "storage term," representing neutrons that have reached thermal equilibrium with the moderator nuclei before emerging. This function fits the pulse shapes of polyethylene moderators very well and the wavelength

dependence of the parameters is

$$\begin{aligned} \Sigma_s &= (S_1^2 + S_2^2\lambda^2)^{1/2}, \quad S_1, S_2 \; constant, \\ \beta &= constant, \\ R &= e^{-E/E_o}, \qquad E_o = constant. \end{aligned} \tag{2.6}$$

It will be shown in a later section the IC function does not work as well for the pulse shapes of liquid methane moderators.

Kropff, Granada, and Mayer [16] mention some other empirical functions used to fit moderator pulse shapes and they will be just briefly mentioned here. These functions however, contain little of the physics of neutron moderation. Windsor and Sinclair [18] used a function with two Gaussians joined at the top. Day and Sinclair [19] convolute an isosceles triangle resolution term with the product of a decaying exponential and step function. Cole and Windsor [20] constructed a function of three sections that smoothly joins two Gaussians and a decaying exponential.

This section has illustrated some of the reasons why pulse shape fitting functions are necessary, to describe some of the physical principles of neutron slowing-down theory fitting functions are created to imitate, and to present a brief history of their development. Work in this field is continuing. The next section presents a generalized version of the IC function recently developed.

2.3 The Generalized Ikeda-Carpenter Function

As was mentioned in the last section, the Ikeda-Carpenter function was the first function used in attempting to fit the liquid methane moderator pulse shape data collected for this thesis. It will be shown in Chapter 4 substantial systematic

deviations were seen when this function was fitted to the liquid methane data. A modification of the IC function was developed so a better representation of the liquid methane moderator pulse shapes might be obtained.

Carpenter [21] has suggested a generalization of the exponent in the slowing-down term ($(at)^2e^{-at}$) from 2, which arises in the theory of neutrons slowing down in an infinite medium of free protons. In the real situation there are molecular effects which complicate the slowing-down process. Sachs and Teller [22] developed the concept of an "effective mass" which would approximate the masses of nuclei in a liquid, where molecular effects can be important, with gas atoms of mass greater than their physical mass. Accounting for the Sachs-Teller effective mass in approximating neutron moderation lends theoretical support for the generalization of the IC function.

Replacing the term 2 in the slowing-down term with a parameter, ν, required additional mathematical work in the convolution of the functions $(at)^\nu e^{-at}$ and $e^{-\beta t}$. A brief summary of Carpenter's derivation follows.

The convolution is performed using Laplace transform techniques and facilitated by representing the needed function as

$$f(t) = \int_0^\infty f_1(t')f_2(t-t')\,dt', \tag{2.7}$$

with

$$f_1(t) = N_1 e^{-\beta t}, \qquad t \geq 0 \tag{2.8}$$

and

$$f_2(t) = N_2(at)^\nu e^{-at}, \qquad t \geq 0 \tag{2.9}$$

where N_1 and N_2 are normalizing factors. The Laplace transform is

$$F(S) \equiv L[f(t)] = \int_0^\infty e^{-St} f(t)\, dt = F_1(S)F_2(S), \tag{2.10}$$

where

$$F_1(S) = L[f_1(t)] = N_1(S+\beta)^{-1} \tag{2.11}$$

and

$$F_2(S) = L[f_2(t)] = N_2\Gamma(\nu+1)a^\nu(S+a)^{-(\nu+1)}. \tag{2.12}$$

The inverse Laplace transform of the product $F(S)$ is

$$f(t) = N_1N_2a^\nu(a-\beta)^{-(\nu+1)}e^{-\beta t}\gamma(\nu+1,(a-\beta)t), \tag{2.13}$$

with

$$N_1 = \beta \tag{2.14}$$

and

$$N_2 = \frac{a}{\Gamma(\nu+1)}. \tag{2.15}$$

The resultant generalized IC function has the form

$$i(v,t) = (1-R)\psi(a,\nu,t) + RF(a,\beta,\nu,t), \tag{2.16}$$

which is the weighted sum of the slowing-down term

$$\psi(a,\nu,t) = \frac{a}{\Gamma(\nu+1)}(at)^\nu e^{-at}, \tag{2.17}$$

and the storage term

$$F(a,\beta,\nu,t) = \frac{\beta a^{\nu+1}}{\Gamma(\nu+1)}(a-\beta)^{-(\nu+1)}e^{-\beta t}\gamma(\nu+1,(a-\beta)t). \tag{2.18}$$

This function has five wavelength-dependent parameters and requires the evaluation of gamma function and incomplete-gamma function components in its computation.

The results of fitting this function to the pulse shape data collected from two liquid methane moderators at the IPNS will be presented in Chapter 4.

3 PULSE SHAPE MEASUREMENTS

In this chapter, the work completed in the collection of moderator neutron pulse shapes is presented. A time-focused crystal spectrometer arrangement was used with a cooled Ge monochromator crystal to select neutrons of discrete wavelengths for analysis. At the time these data were collected, IPNS was producing neutrons with the depleted uranium target. Two heterogeneously poisoned liquid-methane moderators and one grooved solid-methane moderator were in use. Each of these topics will be addressed in the following sections. Much of the discussion was taken from a progress report [23].

3.1 Experimental Details

The measurement of moderator neutron pulse shapes requires a crystal spectrometer arrangement to select neutrons of discrete wavelengths. This allows examination of the intensity of neutrons, of a particular wavelength, leaking from the moderator as a function of time following the source pulse. The time resolution of the pulse shape may then be decoupled from the wavelength resolution. In addition, it is desirable to decouple spatial and angular resolution of the pulse shape when performing a measurement through a technique called time focusing.

The experimental procedure follows closely that outlined by Ikeda and Carpen-

ter when they made similar measurements of polyethylene moderators at IPNS [17], [24]. Figure 3.1 [17] shows the experimental arrangement.

Neutrons behave as waves as well as particles so they are diffracted by the interatomic planes of a crystal according to the Bragg scattering relation. A monochromator crystal and detector are arranged with a Bragg angle, θ_B. The wavelengths reflected by the crystal and visible to the detector are

$$\lambda_n = \frac{2d}{n} \sin\theta_B, \quad n = 1, 2, \cdots \tag{3.1}$$

where n is the order of reflection and d is the interatomic plane spacing.

Time focusing decouples time resolution of a neutron pulse from spatial and angular resolution. This is accomplished by assuring neutrons of each particular order reflection have flight path lengths and Bragg angles (therefore wavelengths and speeds) such that they reach the detector in exactly the same amount of time, regardless of position of origin on the moderator, position and angle of the scatterer from the crystal, and positions of interactions in the detector. A time-focused experimental arrangement provides pulse shape data with much better resolution than could be obtained in an unfocused experiment. The geometric conditions for time focusing must satisfy the following relations (with distances and angles in reference to Figure 3.1);

$$\begin{aligned} P &\equiv L_f / L_i, \\ \tan\ \theta_M &= \frac{1}{2}(1+P)\ \cot\ \theta_B, \\ \tan\ \theta_D &= \frac{1}{2}(1+1/P)\ \cot\ \theta_B, \\ \cot\ \theta_C &= \frac{\cos\ \theta_D\ \tan\ \theta_M + \sin\ (2\theta_B + \theta_D)}{2\sin\ \theta_B\ \sin(\theta_B + \theta_D)}. \end{aligned} \tag{3.2}$$

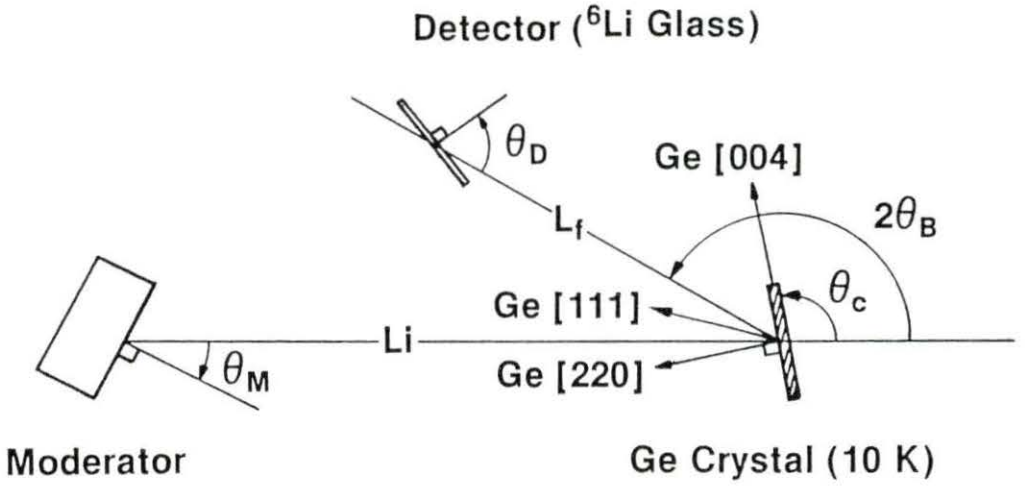

Figure 3.1: Time-focused experimental arrangement for pulse shape measurements

The monochromator was a 1-mm thick, 25-mm diameter Ge crystal cut parallel to (1, 1, 0) planes. The reflecting planes used were the (1, 1, 1) planes. Thus, the reflecting planes were not parallel to the physical plane of the cut face. In such a situation, the relation between the crystal orientation and the Bragg angle is

$$\theta_C = \theta_B + \cos^{-1}\left(\frac{\mathbf{S}\cdot\mathbf{R}}{|\mathbf{S}||\mathbf{R}|}\right), \tag{3.3}$$

where **S** and **R** are the plane normal designations for the physical and reflecting planes, respectively. In each moderator pulse shape measurement, the Bragg angle was θ_B=60°. Each of the beam ports used views its moderator at the angle θ_M=18°. The detector was a 2-mm thick, 75-mm diameter ^{6}Li glass scintillator and was placed to intercept neutrons scattered at $2\theta_B$=120°. For the highest neutron intensity it is desirable to have as short a flight path as possible. This is not always a realizable situation, given the presence of other instruments and equipment in the beamline. The monochromator was always placed downstream of the permanent beamline instruments so flight paths were longer than desired. For each measurement the flight path lengths L_f and L_i were chosen such that their ratio, P, was equal to 0.1. For example, for the F-moderator the crystal was positioned at a distance of L_i = 13.44 m from the face of the moderator and the detector was positioned at a distance L_f = 1.34 m from the crystal. This flight path ratio corresponds to a crystal angle, θ_C=95°, and a detector angle, θ_D=73°. The parameters of the time-focused crystal spectrometer for these measurements are summarized in Table 3.1.

The diamond cubic crystal structure of germanium is such that certain reflections of Ge(n,n,n) for neutrons are not allowed. The allowed reflections of Ge(n,n,n) and their corresponding neutron wavelength, energy, and velocity are

Table 3.1: Parameters of the time-focused crystal spectrometer

$\mathbf{S}=[1, 1, 0]$
$\mathbf{R}=[1, 1, 1]$
$\cos^{-1}\left(\frac{\mathbf{S}\cdot\mathbf{R}}{\lvert\mathbf{S}\rvert\ \lvert\mathbf{R}\rvert}\right) = 35.26^{o}$
$\theta_M=18^{o}$, $\theta_B=60^{o}$
$\theta_D=73^{o}$, $\theta_C=95.3^{o}$
$L_i=13.44$ m, $L_f=1.34$ m ("F" moderator, eVS beam)
$L_i=8.64$ m, $L_f=0.864$ m ("H" moderator, GLAD beam)
$L_i=7.93$ m, $L_f=0.793$ m ("C" moderator, SAD II beam)

presented in Table 3.2. The Ge crystal was mounted in an evacuated test chamber and cooled to about 30 K to increase high-order reflectivity and increase intensity. The refrigeration and vacuum equipment used, however, did not operate consistently and there was warming over the course of each of the data collection runs of at least 10 K.

Data acquisition involved using a PDP-11 instrument computer system operating in time-of-flight sorting mode. Neutron detection events are sorted into time bins corresponding to the neutron time of flight following the source pulse. In this way, a histogram of neutron events as a function of time is created. These histograms or time-of-flight spectra contain the crystal reflection peaks (pulse shapes) used in the pulse shape analysis.

3.2 The Liquid Methane F- and H-Moderators

The liquid methane moderators in use at IPNS are contained in aluminum cans having nominal dimensions of 10 x 10 x 5 cm^3 and are located within the graphite-beryllium reflector assembly in close proximity to the neutron producing

Table 3.2: Allowed reflections of Ge(n,n,n)

n	λ (Å)	E_n (meV)	v (ms^{-1})
1	5.6859	2.53	695.8
3	1.8953	22.8	2087
4	1.4215	40.5	2783
5	1.1372	63.3	3479
7	0.8123	124	4871
8	0.7107	162	5567
9	0.6318	205	6262
11	0.5169	306	7654
12	0.4738	364	8350
13	0.4374	428	9046
15	0.3791	569	10437
16	0.3554	648	11133
17	0.3345	731	11829
19	0.2993	913	13220
20	0.2843	1012	13916
21	0.2708	1116	14612

target. Each moderator is surrounded by a layer of a boron-aluminum composite. The absorber "decouples" the moderator from the reflector by absorbing thermal neutrons attempting to enter the moderator. Since the relaxation time of thermal neutrons in graphite is about 200 μs, these neutrons would lengthen the pulse if they entered the beam. The decoupler helps to provide shorter pulses. The moderators are part of a circulating liquid-methane cooling system which cools the methane to a temperature of about 100 K.

Pulse width resolution requirements vary among instruments. The F moderator is heterogeneously poisoned with a 0.5 mm-thick gadolinium foil 1.7 cm below both of the viewed surfaces. Gadolinium is a neutron absorber and serves to reduce the neutron pulse width for long wavelengths, a desirable condition for those instruments which require good pulse width resolution. The H moderator is poisoned with a single layer of gadolinium located at 2.5 cm below its one viewed surface. Pulse widths are shortened in the same manner as above. Gadolinium has a large absorption cross section for the long-lived thermal component in the moderator. Instruments on the H-moderator beams have resolution requirements which are not as severe as for those which use the F moderator.

Pulse shape measurements were made, using the time-focused, cooled-crystal spectrometer arrangement described in the previous section, during the summer of 1987 for the F moderator and during the spring of 1988 for the H moderator. Much experience has been gained in the experimental technique of pulse shape measurement over the course of this work as evidenced by comparing the quality of data obtained from each moderator.

From the neutron time-of-flight spectra obtained for the F moderator, "good" data ("good" meaning that statistical fluctuations do not distort or mask the pulse shape) were available through the ninth order reflection (205 meV) and reflections were observed through the 16th order (648 meV). There are several factors contributing to the low count rates in this measurement, including the diminishing beam intensity for this long path length (14.78 m from moderator to detector), and problems with cooling, vacuum, and beam alignment.

Figures 3.2, and 3.3 respectively illustrate raw data from the F moderator,

Ge(3, 3, 3), and Ge(4, 4, 4) reflections. The Ge(4, 4, 4) reflection has the best counting statistics of the F moderator measurement with nearly 1,500 counts in the peak channel. These high resolution measurements immediately reveal the very sharp rise in the leading edge, which is characteristic of neutron moderation in methane. In the case of Figure 3.2 the 10-90 % rise time is about eight microseconds, a relative wavelength resolution of about 0.1 % at this flight path length.

From the neutron time-of-flight spectra obtained for the H moderator, good data were available through the 16th order reflection (648 meV) and reflections were observed through the 21st order reflection (1.12 eV). There are nearly twice as many counts in the peak channel of the H moderator Ge(16, 16, 16) reflection as there are in the most prominent reflection from the F moderator data. The quality of these data is much improved over those of the F moderator because intensity increased for the shorter flight path length (9.50 m from moderator to detector), the improved experimental apparatus performance, and the benefit of gained experience in making pulse shape measurements.

Figures 3.4, and 3.5 respectively illustrate raw data from the H moderator, Ge(1, 1, 1), and Ge(4, 4, 4) reflections. The fourth-order reflection has the best counting statistics of the H moderator measurement with nearly 150,000 counts in the peak channel (an increase over the F moderator measurement by a factor of about 100).

Small peaks are present in the raw data corresponding to Ge(2, 2, 2) and Ge(6, 6, 6) reflections in both the F and H measurements. Additionally, there is a small peak corresponding to the Ge(10, 10, 10) reflection in the H moderator data. As noted by Ikeda and Carpenter [17], these reflections are prohibited in the dia-

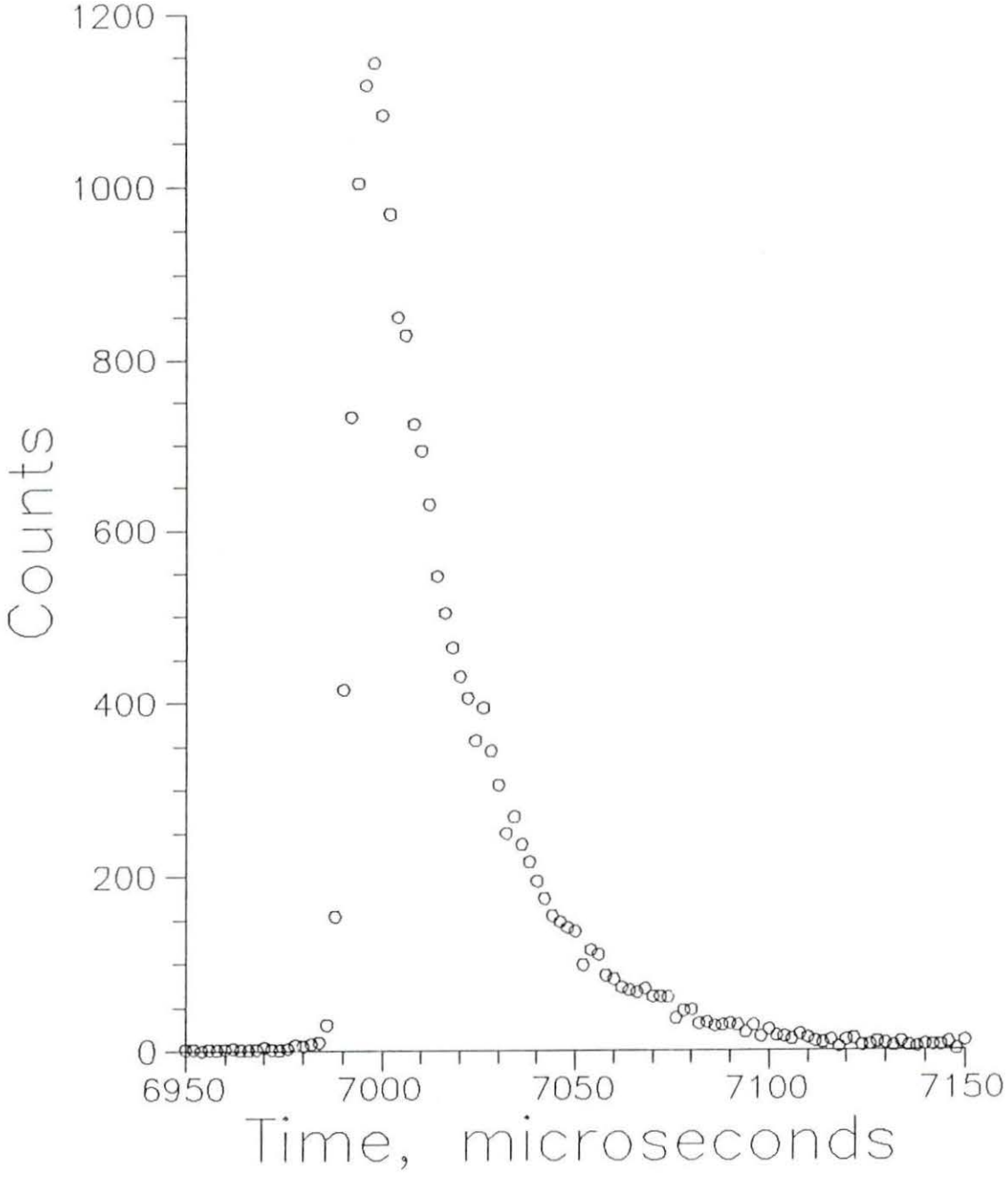

Figure 3.2: Ge(3,3,3) reflection observed in F moderator measurement. The neutron energy is 22.8 meV

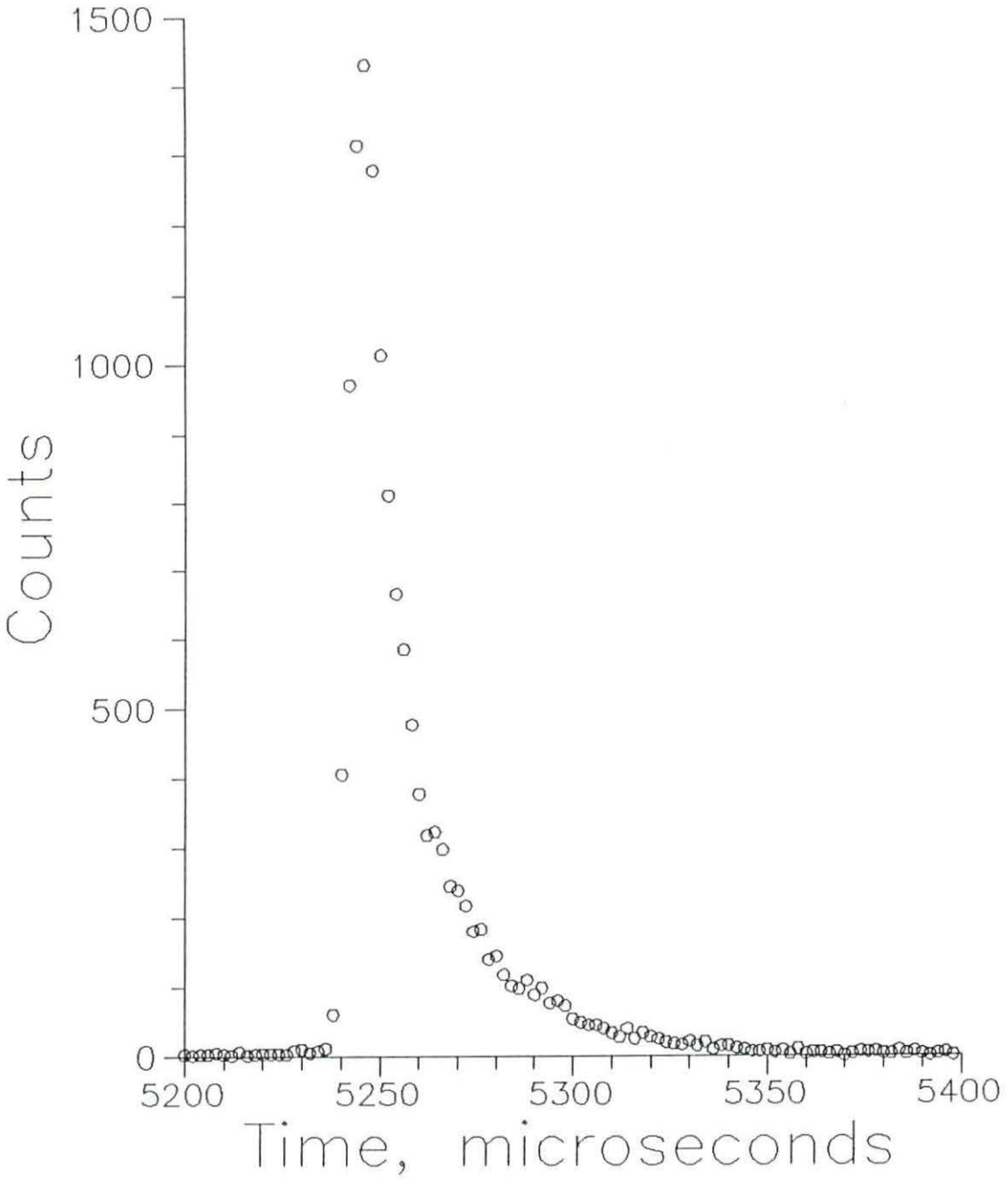

Figure 3.3: Ge(4,4,4) reflection observed in F moderator measurement. The neutron energy is 40.5 meV

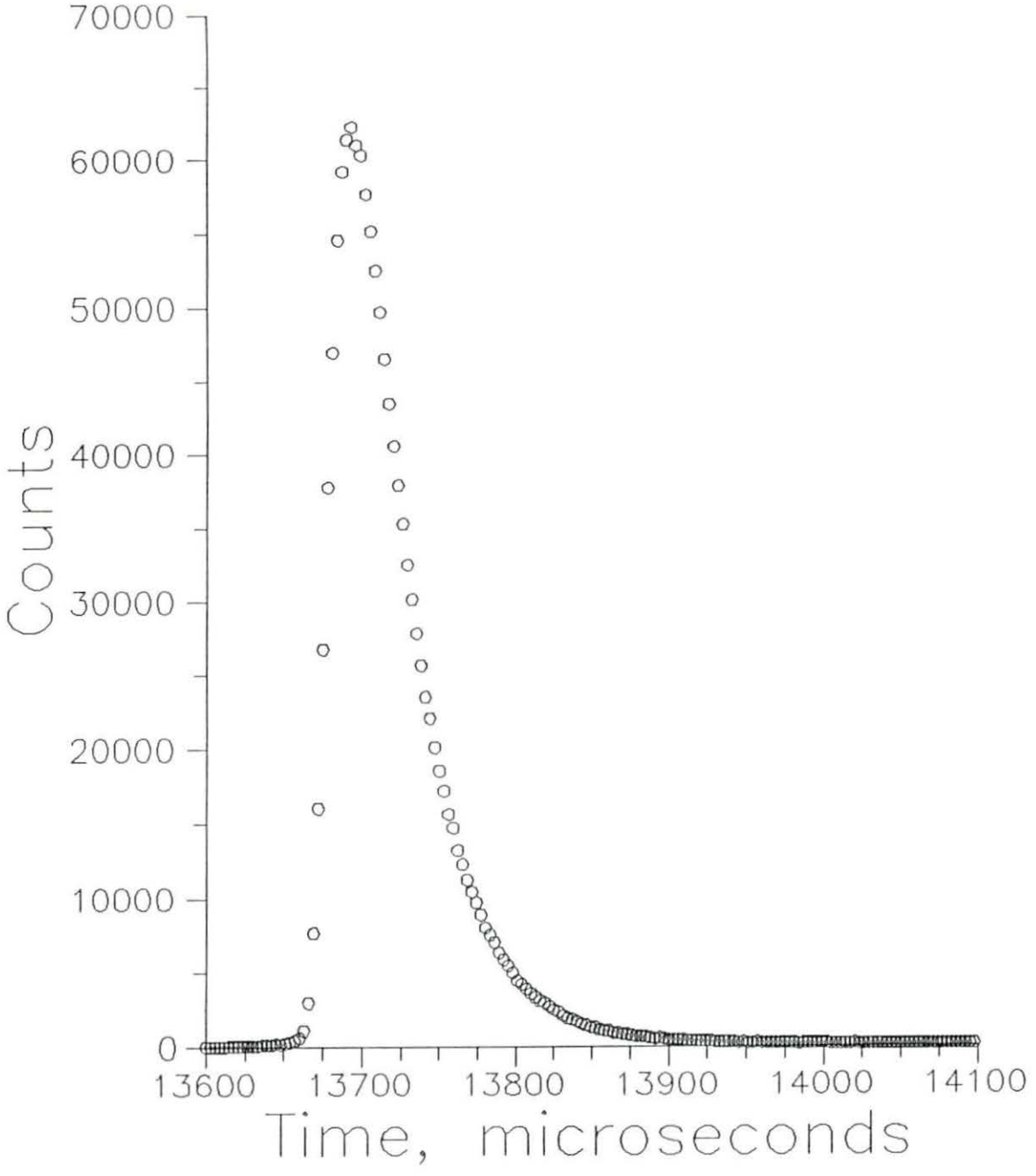

Figure 3.4: Ge(1,1,1) reflection observed in H moderator measurement. The neutron energy is 2.53 meV

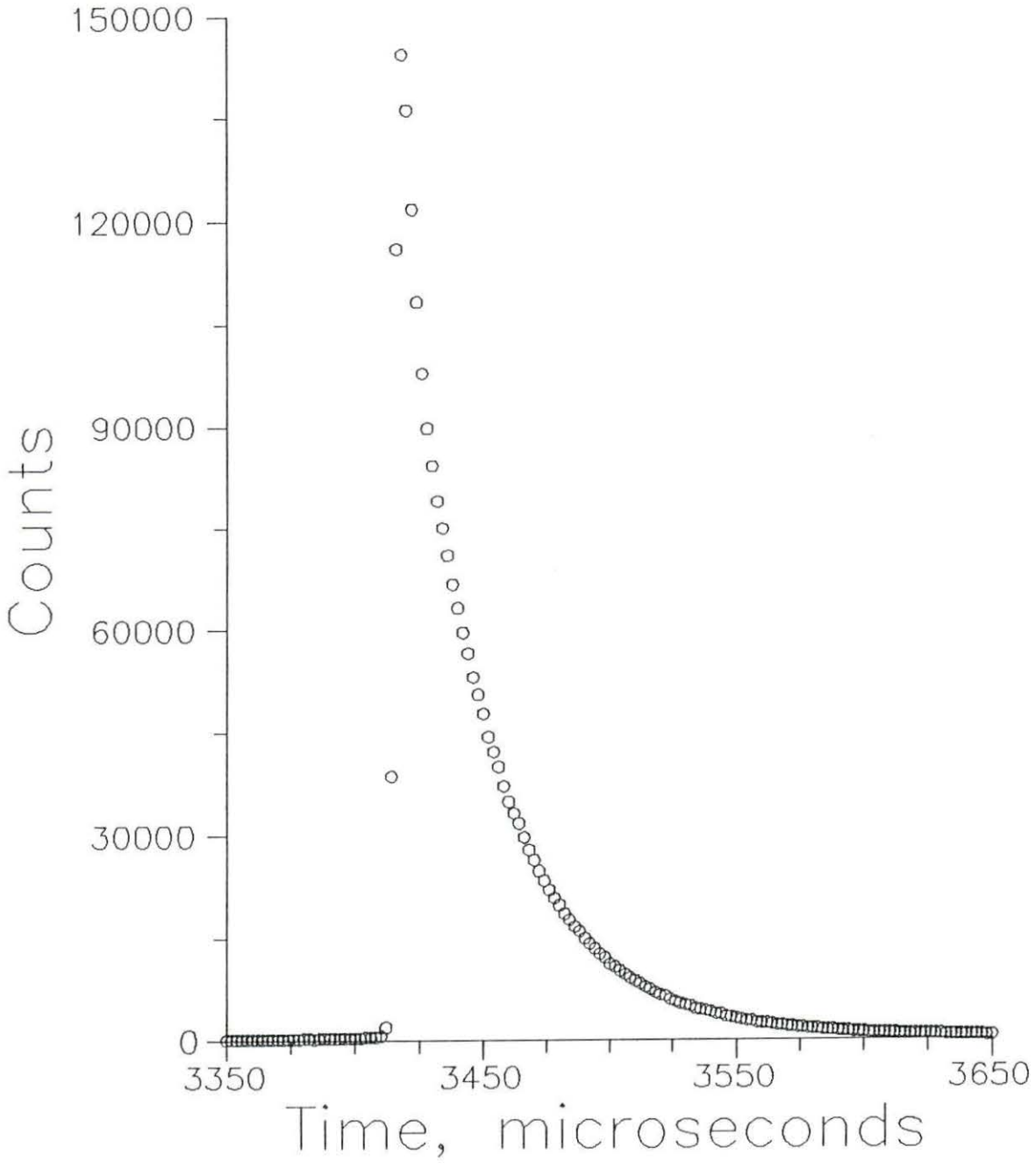

Figure 3.5: Ge(4,4,4) reflection observed in H moderator measurement. The neutron energy is 40.5 meV

mond crystal structure of germanium, but are presumably caused by imperfections of the crystal due to impurities or strains.

One indication of the performance of a pulsed moderator is the full width at one-half maximum (FWHM) of the neutron pulse. Figure 3.6 shows the FWHM of neutron pulses obtained from the raw data. Visible in this figure is the effectiveness of the Gd poisoning as a function of neutron energy. The additional poisoning present in the F moderator serves to decrease the widths of neutron pulses for long wavelengths.

Another method of illustrating the time and energy dependence of neutron pulse shapes is shown in Figures 3.7 and 3.8. These figures respectively show several measured pulse shapes for the F and H moderators, normalized to unity at the peak. The time scale has been replaced by a length scale by multiplying the emission time $t - t_0$ following the source pulse at time t_0, by the neutron speed v. This length scale is called the "reduced time" and such a representation of the pulse shapes gives directly the resolution attained for a given flight path length [4]. Each curve in Figures 3.7 and 3.8 represents a slice of the third dimension of a moderator neutron pulse shape: energy. Two main features characteristic of pulsed moderators are apparent in these figures. For epithermal neutron energies, the neutron pulse shape expressed as a function of (vt) is nearly invariant with energy as expected because the neutron flux per unit energy of a slowing-down spectrum has a $1/E$ dependence. For lower energies, the neutron pulse shape maintains a fast rise time but has a decaying exponential tail characteristic of a Maxwellian flux distribution. These figures also show clearly the resolution may be improved if either the Maxwellian "bulge" in the pulse shape can be moved to lower energies

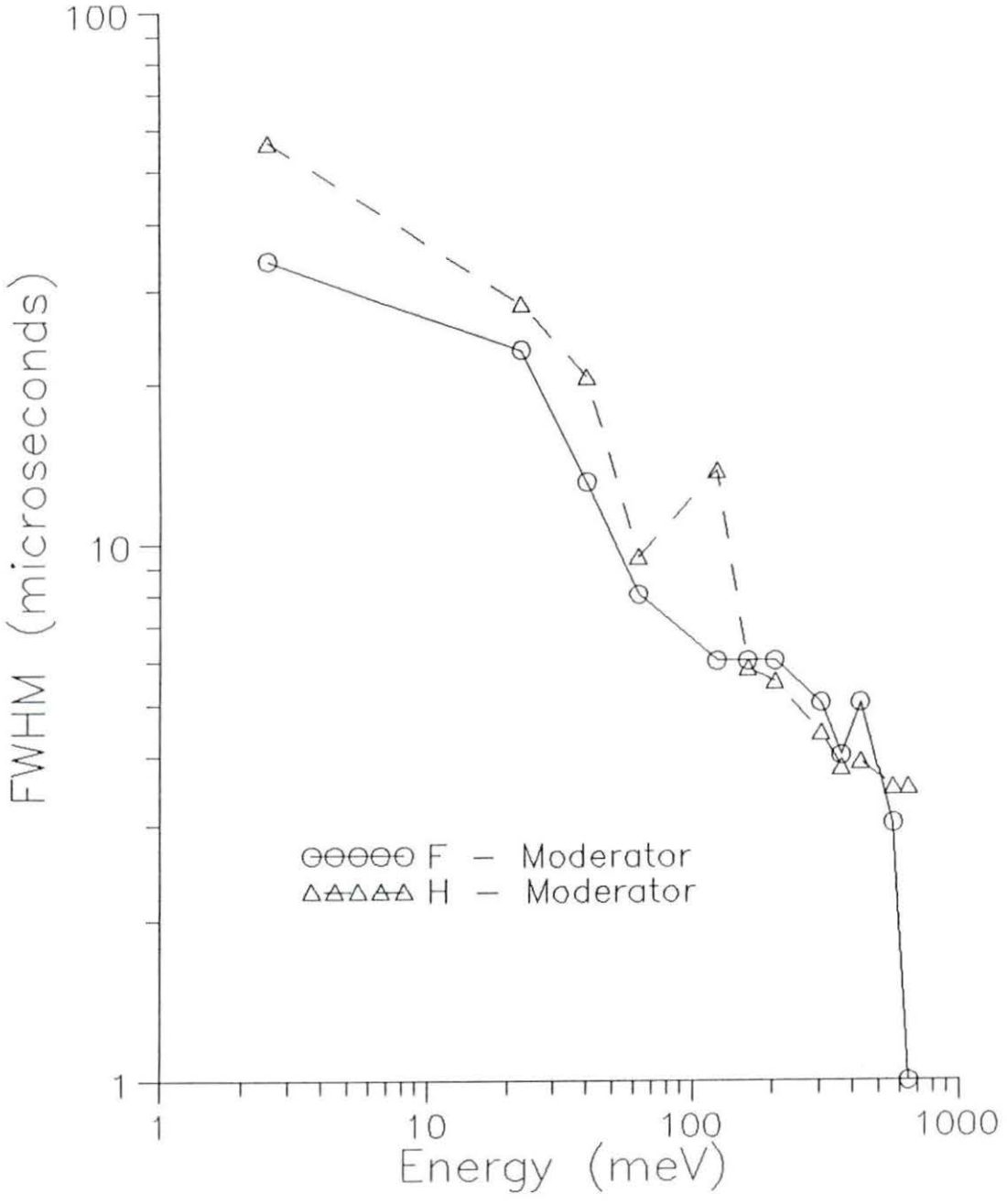

Figure 3.6: Neutron pulse widths of the H and F moderators; symbols are observed values in both measurements

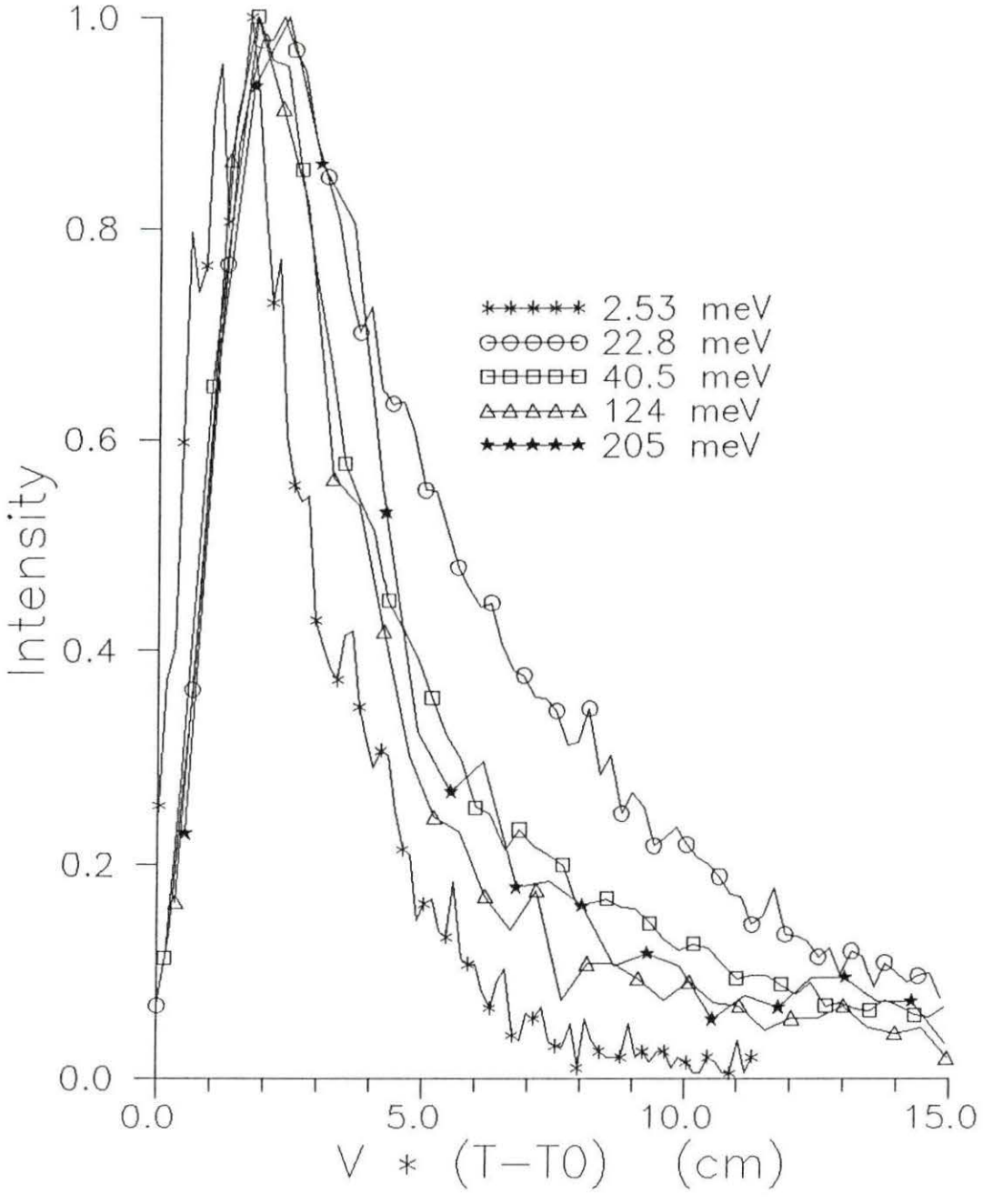

Figure 3.7: F moderator normalized neutron pulse shapes for several energies; the abscissa is a reduced time scale $v(t-t_0)$, where v and t_0 are the neutron speed and the beginning time of the neutron pulse

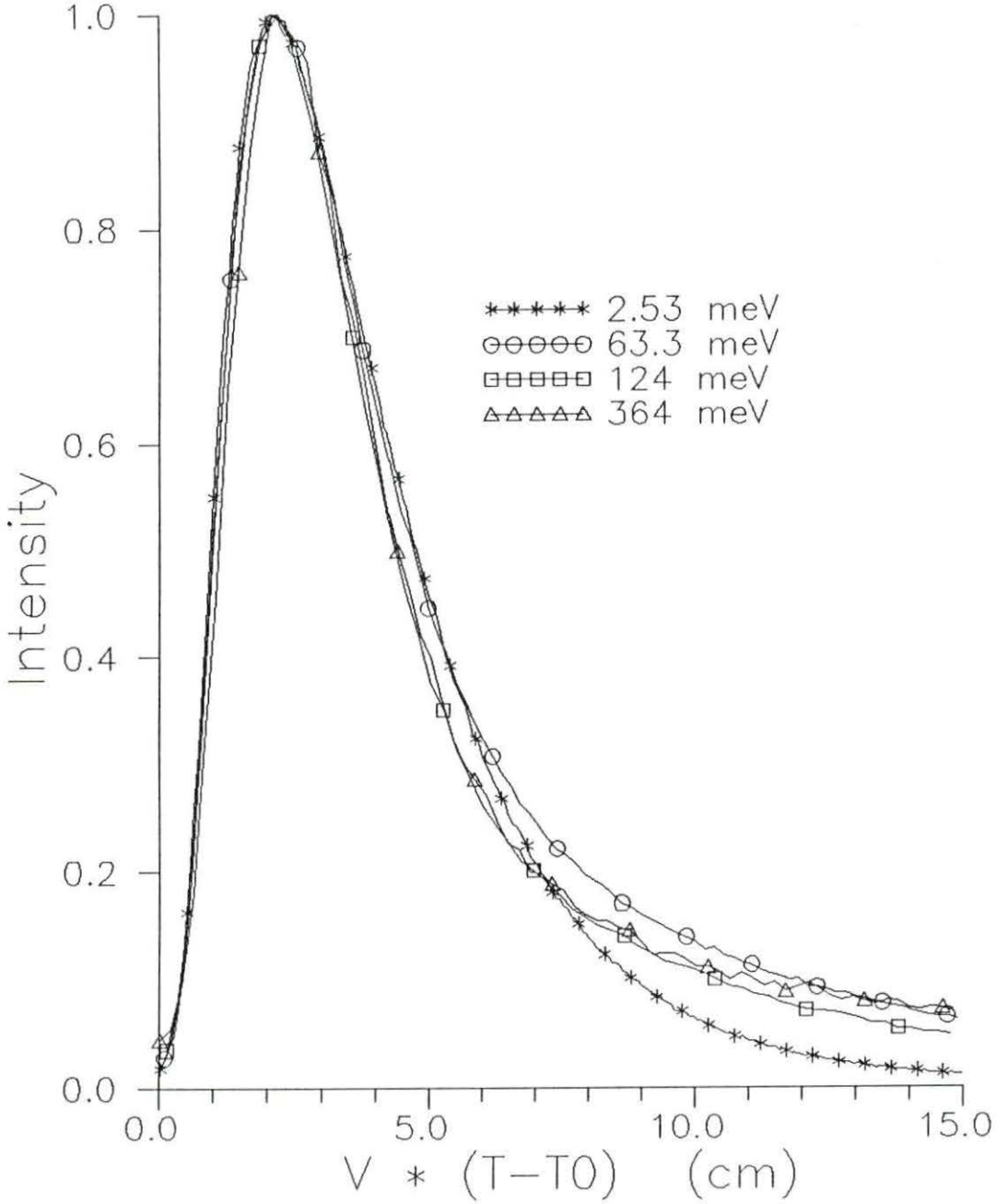

Figure 3.8: H moderator normalized neutron pulse shapes for several energies; the abscissa is a reduced time scale $v(t-t_0)$, where v and t_0 are the neutron speed and the beginning time of the neutron pulse

(by cooling the moderator) or if the exponential decay time of the Maxwellian tail can be reduced (by adding heterogeneous poisons).

Measurements such as those described here for the liquid methane F and H moderators at IPNS provide the data necessary for the analysis of moderator neutron emission-time distributions using fitting functions. Results of this analysis for the F and H moderators will be presented in the next chapter.

3.3 The Grooved Solid Methane C-Moderator

Adding heterogeneous poisons to a moderator improves resolution but reduces neutron intensity. Cooling a moderator will push the Maxwellian component of a moderator pulse to lower energy but will result in a loss of neutron intensity in the region of the moderator where a warmer Maxwellian would be. Thus, resolution and intensity requirements are often in conflict in pulsed neutron research.

There are applications for pulsed neutron sources that do not have a severe requirement for high resolution but do need greater intensity. For this reason, the IPNS has used a grooved solid methane moderator (the "C" moderator) which provides a greater intensity of long wavelength neutrons, albeit poorer resolution, than the liquid methane moderators.[1] Measurements of the pulse shapes of the C moderator were made during the fall of 1987 by the same method described previously. Examples of the pulse shapes of the C moderator are presented in this section.

The IPNS grooved solid-methane C moderator is shown in Figure 3.9 [25]. Like

[1]Since the time that measurements for this thesis were performed, the IPNS grooved solid-methane C moderator has been replaced with a liquid hydrogen moderator.

its liquid-methane counterparts, it has nominal overall dimensions of 10 x 10 x 5 cm^3 and is decoupled from the reflector by a layer of a boron-aluminum composite. The aluminum moderator can contains an aluminum foam which conducts neutron- and gamma-ray-deposited heat outward from the moderator interior. The moderator is filled with methane and cooled with liquid helium to a temperature of 15 K. The result is a grooved volume of solid methane.

From the neutron time-of-flight spectra for the C moderator, good data were available through the 12th order reflection (364 meV) and reflections were observed through the 16th order reflection (648 meV). Figure 3.10 illustrates raw data from the C moderator Ge(4, 4, 4) reflection. The most obvious difference in the pulse structure between grooved and flat moderators is the "shoulder" present on the leading edge of grooved moderator pulses. This feature arises because neutrons emerge from the tips of the fins as well as the bottoms of the grooves and there is a time delay required for the neutrons to travel the length of the fins. It is apparent that neutron intensity is greatest from the bottoms of the grooves.

Analysis of the neutron pulse shapes of grooved moderators is more complicated than that of flat moderators because the resultant pulse is the sum of two separated sources (the fins and the grooves). Because of the more complicated nature of grooved moderator analysis and the fact that instruments which utilize grooved moderators do not have severe resolution requirements, data analysis of the C moderator was given lowest priority. There is no mention of the C-moderator data in the chapter describing the data fitting process.

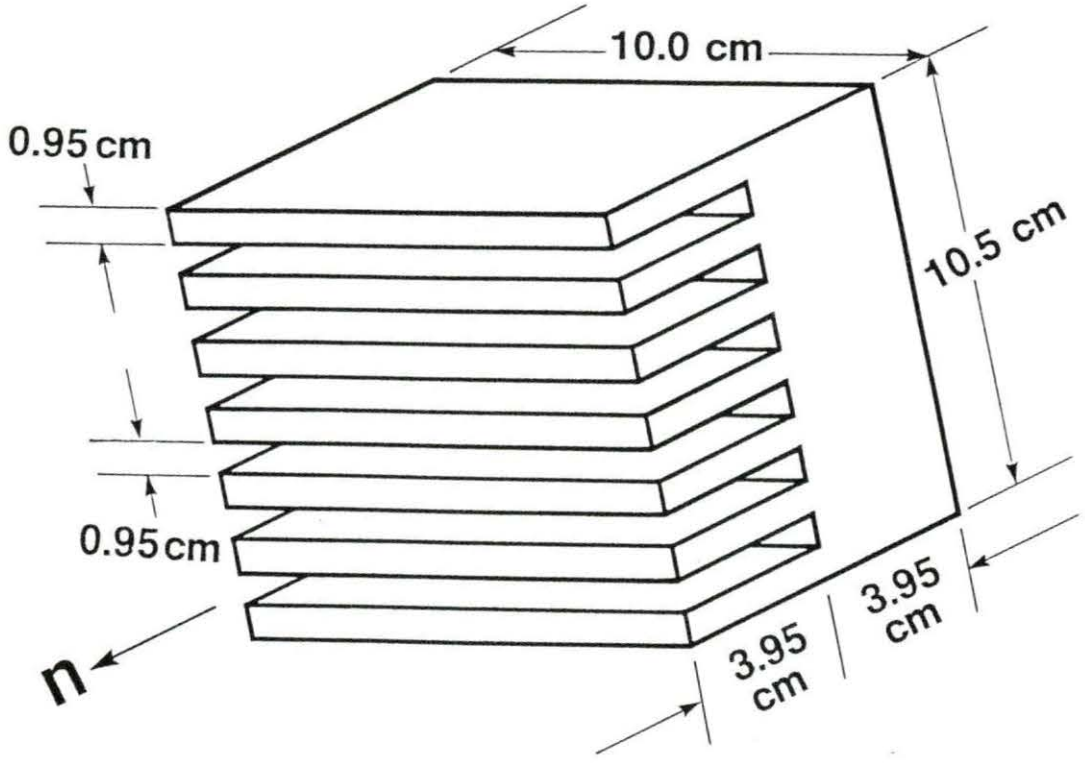

Figure 3.9: The IPNS grooved solid methane C moderator

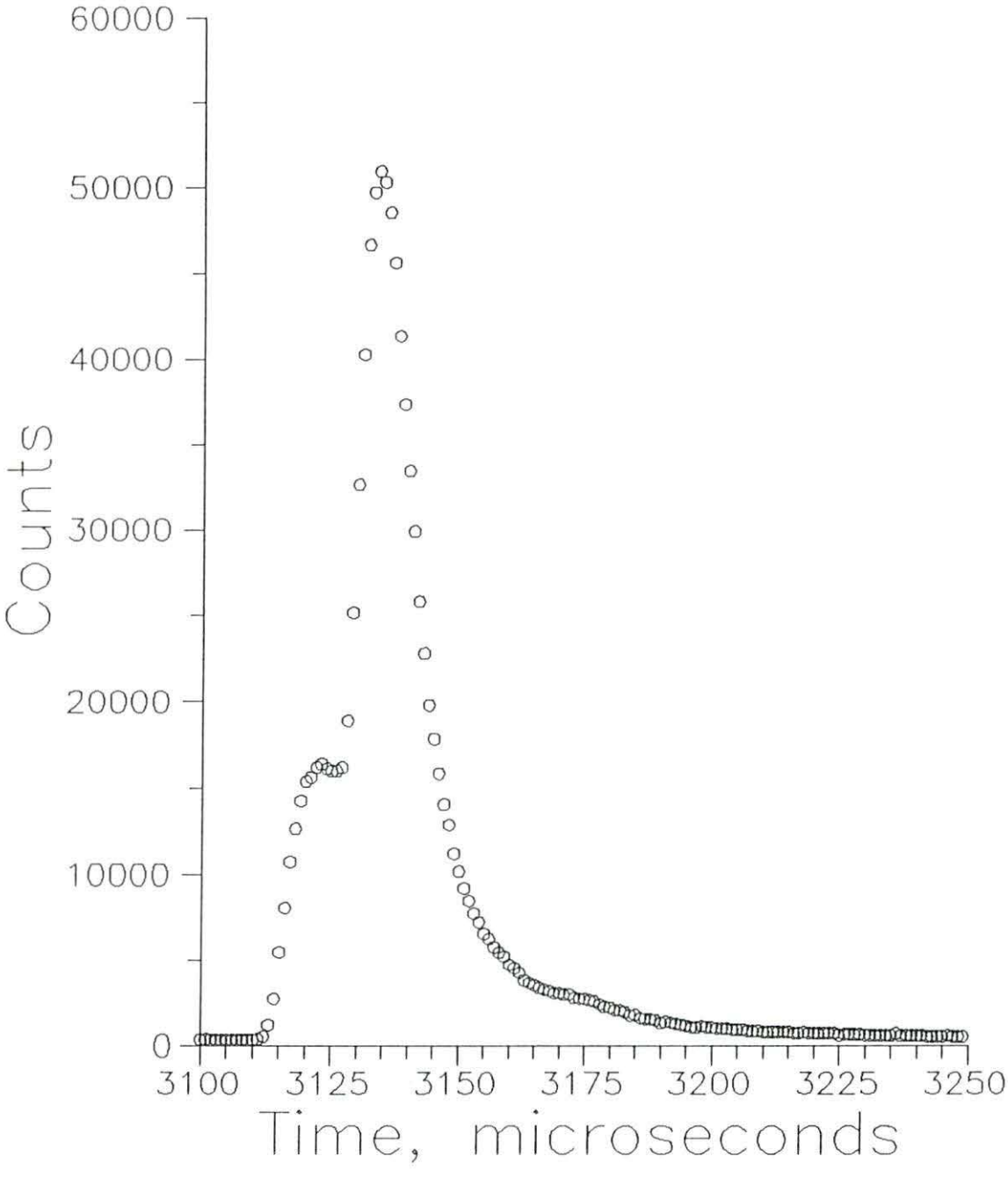

Figure 3.10: Ge(4,4,4) reflection observed in C moderator measurement, E= 40.48 meV

4 DATA ANALYSIS AND DISCUSSION

The analysis of data from pulse shape measurements requires the use of computer routines to fit pulse shape fitting functions to the data. The fitting functions discussed previously are all nonlinear. Computer routines utilizing nonlinear least squares algorithms are necessary to evaluate the functional parameters providing best fits to the data.

This chapter begins with a brief discussion of the curve fitting techniques used in the data analysis. This is followed by sections presenting results of data analysis using the Ikeda-Carpenter function, showing the systematic deviations suggesting the need for its generalization, and results of analysis using the generalized IC function. The latter section additionally illustrates the observed wavelength dependence of the generalized IC function parameters.

4.1 Curve Fitting

The analysis of pulse shape data begins with deciding upon a fitting function which hopefully approximates the functional relationship between the variables y and t (that is, between the quantities of neutron counts per time channel and time). Once an appropriate fitting function is chosen, a method is needed to determine the values of the functional parameters which provide the best representation of the

data. The method used is the least squares method applied to nonlinear functions. To describe the application of the nonlinear least squares method it is necessary to introduce some notation and theory of nuclear counting statistics.

Let $g(t_i,\mathbf{a})$ be the value of the function evaluated at time t_i following the source pulse of fast neutrons, given the vector $\mathbf{a}$ of functional parameters. Let y_i be the net number of counts recorded over a time interval Δt which begins at time t_i following the source pulse. The net number of counts over a time interval is determined by taking the total number of counts detected over the interval and subtracting an estimate of the background over the interval. Background is estimated by computing an average value of the observed data in a region before and after each pulse shape to be analyzed. The equation of a straight line between these points serves to define the amount of background to be subtracted from the observed data in each time interval.

The *ith* residual, or the deviation between the net number of counts at time t_i and the value of the function evaluated at time t_i is expressed as

$$f_i(\mathbf{a}) \;=\; y_i \;-\; g(t_i,\mathbf{a}). \tag{4.1}$$

The method of least squares optimizes the estimates of the parameters in $\mathbf{a}$ by minimizing the sum of the squares of the residuals over all t_i for a pulse shape. The problem, then, is to seek a solution vector, $\mathbf{a}'$, which produces the minimum sum of squares of residuals. This may be expressed as

$$min\left[\sum_{i=1}^{n} f_i(\mathbf{a})^2\right] \;=\; \sum_{i=1}^{n} f_i(\mathbf{a}')^2. \tag{4.2}$$

The method of least squares defined above inherently assumes each data point, y_i, has equal variance. If the variances are not equal, it becomes necessary to

introduce a weighting factor into the calculation of the residual sum of squares. The number of counts recorded by a detector in a unit time interval has a statistical uncertainty proportional to its magnitude. If the same measurement in a counting experiment was made repeatedly, the observed values would be distributed about their mean in a Poisson distribution [26]. In Poisson statistics the variance of an observation is

$$\sigma_i^2 = y_i. \tag{4.3}$$

It is then possible to define a weighted-residual sum of squares as

$$\sum_{i=1}^{n} \frac{1}{\sigma_i^2} f_i(\mathbf{a})^2 = \sum_{i=1}^{n} \frac{1}{y_i} [y_i - g(t_i, \mathbf{a})]^2, \tag{4.4}$$

which accounts for the statistical uncertainties in the counting measurement.

Computer code packages are available containing algorithms for performing least squares curve fitting with nonlinear functions. The MINPACK-1 package, developed by Moré, Garbow, and Hillstrom [27] was used extensively in the data analysis. MINPACK-1 subprograms solve nonlinear least squares problems by using a modification of the Levenberg-Marquardt algorithm. This algorithm adjusts components of the parameter vector, $\mathbf{a}$, by adding internally derived correction factors to each parameter, and recalculating the residual sum of squares. The process is continued until one of several convergence tests are satisfied, indicating the solution vector, $\mathbf{a}'$, has been found. When used in conjunction with a user supplied driver program and subroutines for evaluating the fitting function, MINPACK-1 supplies as output the evaluated functional values at each time step, the weighted residual sum of squares, the parameter vector, and the covariance matrix.

Once a solution vector has been evaluated, statistical indices such as parameter

confidence intervals and the coefficient of determination may be calculated [28]. A confidence interval is an interval estimate which asserts with a specified confidence that a parameter lies in the interval. For example, the 95% confidence interval for a parameter a_k, an element of the parameter solution vector, is given by

$$a_k \pm \sigma_k * 1.96, \tag{4.5}$$

where σ_k is the standard deviation of a_k. The coefficient of determination, R^2, provides some measure of the goodness of fit. It is an index of how well the chosen fitting function (the statistical model) accounts for the total variability of the measurement. It may be expressed as

$$\begin{aligned} R^2 &= \frac{variation\ explained\ by\ model}{total\ variation}, \\ R^2 &= \frac{total\ sum\ of\ squares\ -\ residual\ sum\ of\ squares}{total\ sum\ of\ squares}. \end{aligned} \tag{4.6}$$

Examples of the use of these will be shown in Section 4.3 in the analysis of pulse shape data using the generalized IC function.

4.2 The Ikeda-Carpenter Function

The Ikeda-Carpenter function (Equation 2.5) was chosen as the first candidate for the data analysis of this thesis because of its previously demonstrated success at characterizing the pulse shapes of polyethylene moderators [17]. Pulse shapes of the liquid-methane moderator measurements were fitted using the IC function maintaining all parameters of the function, a, β, R, a scale factor, and a time delay t_0 as free parameters for each wavelength. The time delay represents the neutron flight time from moderator to detector plus a fixed shift of the time origin which results

from time offsets in the triggering of electronic timing equipment. The beginning of the pulse shape is defined by t_0.

The results of the curve fitting revealed substantial, systematic deviations of the best fitted functions from the data. These deviations were manifested as underestimation of the height and integral of each peak. Figures 4.1 and 4.2 respectively show examples of the results of fitting the Ge(3, 3, 3) and Ge(4, 4, 4) reflections of the F moderator, illustrating the aforementioned deviations. Figure 4.1 indicates well however, that the slowing-down term is important in determining the rising part of the peak and that the exponentially-decaying storage term is dominant in the tail at this wavelength. At shorter wavelengths the storage term becomes less important. A greater fraction of the pulse is composed of neutrons emerging from the moderator in the process of slowing down, before becoming thermalized.

The results of data analysis using the IC function as illustrated by these two examples indicated a modification of the function was needed. The generalized IC function was derived to fulfill this need. Results of its use in the analysis of the liquid-methane moderator measurements are presented in the next section.

4.3 The Generalized Ikeda-Carpenter Function

The generalization of the IC function resulted in Equation 2.16. Pulse shapes of the liquid-methane moderator measurements were again fitted, but using the generalized IC function maintaining all parameters, a, β, R, a scale factor, t_0, and the exponent parameter ν as free parameters for each wavelength. The results showed improvement over previous fitting in that deviations of the best fitted functions from the data were reduced or eliminated entirely. The resultant parameters,

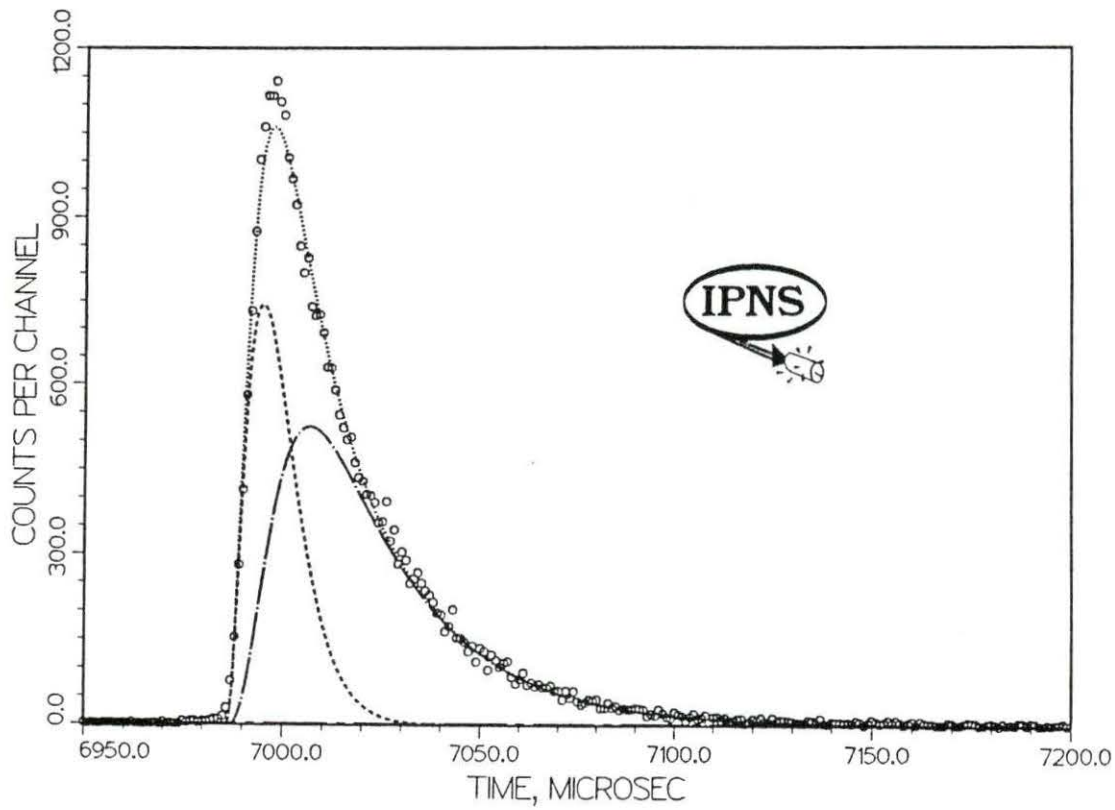

Figure 4.1: Ge(3,3,3) reflection for F moderator. The dotted line is calculated by Equation 2.5

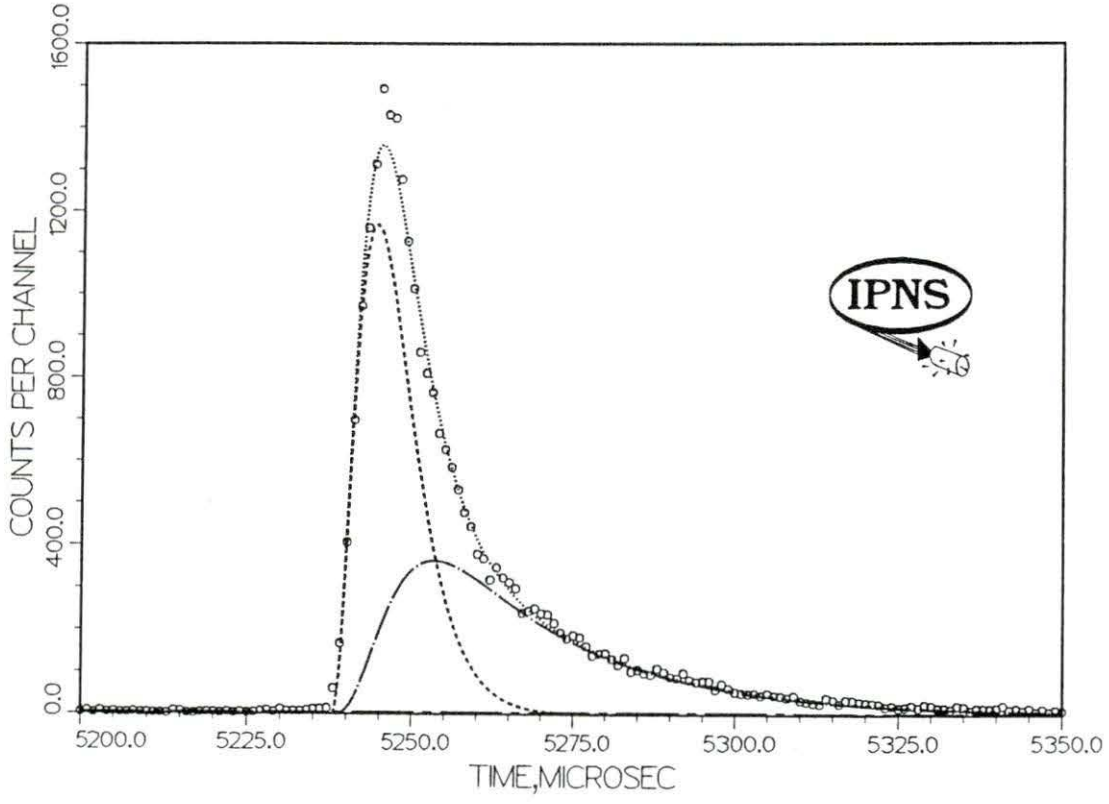

Figure 4.2: Ge(4,4,4) reflection for F moderator. The dotted line is calculated by Equation 2.5

however, displayed some unexpected variation as a function of wavelength. The wavelength-dependence of the parameters was expected to be somewhat similar to that observed for polyethylene as denoted in Equation 2.6. The exponent parameter ν was expected to approach a lower limit of 2 for shorter wavelengths and should in some fashion become greater than 2 for longer wavelengths to account for the Sachs-Teller effective mass. Instead, the parameter had large fluctuations as a function of wavelength. Of particular concern was that the parameter β, expected to be constant, was showing a considerable increase in value with decreasing wavelength.

In least squares analysis, the "parameter space" is searched until a minimum in the residual sum of squares is reached. In parameter space there may exist several sets of parameters corresponding to relative minima in the least squares analysis. If the computer algorithm finds one of these relative minima it will stop its search without locating the true solution vector. The choice of starting values in the analysis is therefore very important.

Several attempts were made at modifying the computer fitting programs to impose a functional form of the wavelength dependence of each parameter and fit, using these constraints, several of the pulse shapes of a measurement "simultaneously." These modifications allowed evaluation of the parameters of the generalized IC function for several peaks using parameter functional forms that should represent the expected physical behavior of the parameters. The final parameters in the wavelength-dependent equations were evaluated by computing and minimizing the sum of the residual sum of squares of all the peaks in the analysis.

The wavelength-dependence equations for the generalized IC function parameters were assumed equivalent to those in Equation 2.6 with the addition of the

following expressions for t_0 and ν

$$\begin{aligned} t_0 &= M\lambda + B, \qquad M,\ B\ \ constant, \\ \nu &= 2. + c^2 exp\left(\frac{-E}{E'}\right), \quad c,\ E'\ \ constant. \end{aligned} \tag{4.7}$$

This representation of the generalized IC function now called for fitting seven wavelength-independent parameters to determine the four wavelength-dependent parameters for each peak and an eighth parameter for the assumed wavelength-independent parameter β. Also included in the fitting was a scale factor for each peak. This method of analysis was not very successful but did demonstrate that wavelength-independence of the parameter β should not automatically be assumed.

A decision was made that the remainder of the data analysis for this thesis should be primarily directed toward showing that good fits of methane moderator pulse shapes could be obtained with the generalized IC function; not necessarily toward developing any new insight into the wavelength-dependence of parameters. A more modest method of data analysis was undertaken which simplified the curve fitting process.

It is desirable in a nonlinear least squares problem to have as few unknown parameters as possible. In the generalized IC function, the parameters whose wavelength dependence is known with the greatest confidence are Σ (and hence, a because $a = v\Sigma$) and t_0. However, in the same sense as ν may deviate from 2 on account of the wavelength variation of the effective scatterer mass, a may deviate from $v\Sigma$ by a wavelength dependent factor. This coupling between ν and a has been ignored in the data analysis. Determining values of these parameters for each peak in a measurement before performing the least squares analysis cuts the number of fitted

parameters to three: β, ν, R, and a scale factor, and results in a major simplification.

The elimination of t_o from the vector of fitted parameters was accomplished for each moderator measurement by examining output of the time-of-flight spectra for four peaks and estimating the start time of each peak. (The very fast rise time of methane moderator pulse shapes facilitated this.) A simple linear regression to evaluate the parameters in the expression $t_0 = M\lambda + B$ was performed on each set of points. For the F moderator, the regression was performed on the n= 3, 4, 5, and 7 peaks becuse they had the most easily discernible start times. The results of the regression were M = 3690.36 μsÅ^{-1} and B = -7.38 μs. For the H moderator, the regression was also performed on the n= 3, 4, 5, and 7 peaks, resulting in M = 2403.84 μsÅ^{-1} and B = -5.46 μs. With these parameters, values of t_0 were calculated for each of the peaks in both moderator measurements.

The elimination of Σ was somewhat more complicated. Three peaks from each moderator measurement were fit simultaneously. The only wavelength-dependent equation of constraint, however, was $\Sigma = (S_1^2 + S_2^2\lambda^2)^{1/2}$. The other parameters were treated as free parameters of wavelength. The result of this calculation was the evaluation of the constants S_1 and S_2, from which values of Σ and a for each of the peaks in both moderator measurements were calculated. The three peaks in each moderator measurement to be fit in this manner were chosen with more emphasis placed on data quality than choosing a wide range of wavelengths. For the F moderator, the fitting was performed on the n= 3, 4, and 5 peaks, resulting in S_1= 1.159 cm^{-1} and S_2= 0.373 $\text{cm}^{-1}\text{Å}^{-1}$. For the H moderator, the fitting was performed on the n= 1, 4, and 5 peaks, resulting in S_1= 1.759 cm^{-1} and S_2= 0.0059 $\text{cm}^{-1}\text{Å}^{-1}$. It is possible that different sets of peaks may have produced

Table 4.1: Fitted parameters for the F moderator

n	t_0 (μs)	a (μs^{-1})	β (μs^{-1})	ν	R (%)	$Coef.\ of\ Det.$
1	20976	0.169	0.0456±0.023	2.00±0.01	72.3±3.4	0.95182
3	6987.0	0.284	0.0427	2.00	74.6	0.98863
4	5238.5	0.355	0.0489	2.02	52.8	0.98814
5	4189.3	0.430	0.0710	2.08	33.2	0.98137
7	2990.3	0.584	0.0832	2.10	31.8	0.96563
8	2615.4	0.662	0.0806	2.55	28.0	0.96781
9	2324.2	0.741	0.107±0.017	2.38±0.17	30.3±5.1	0.94562

different values for S_1 and S_2 but this was not investigated.

The pulse shapes of both moderator measurements were then fitted with the appropriate values of t_0 and a entered as constants while maintaining the parameters β, ν, R, and a scale factor as free parameters of wavelength. Figures 4.3 and 4.4 respectively show results of fitting the F moderator Ge(3, 3, 3) and Ge(4, 4, 4) peaks. There is still some deviation of the best fitted function from the data but there is substantial improvement over best fitted functions of the original IC function.

Figures 4.5, 4.6, and 4.7 respectively show results of fitting the H moderator Ge(1, 1, 1), Ge(4, 4, 4), and Ge(12, 12, 12) peaks. The quality of fits to the measured H moderator pulse shapes is excellent. Tables 4.1 and 4.2 respectively give the fitted parameters of the pulse shapes analyzed in the F and H moderator measurements. For illustration purposes, 95% confidence intervals are given for the parameters of the Ge(1, 1, 1) and Ge(9, 9, 9) peaks.

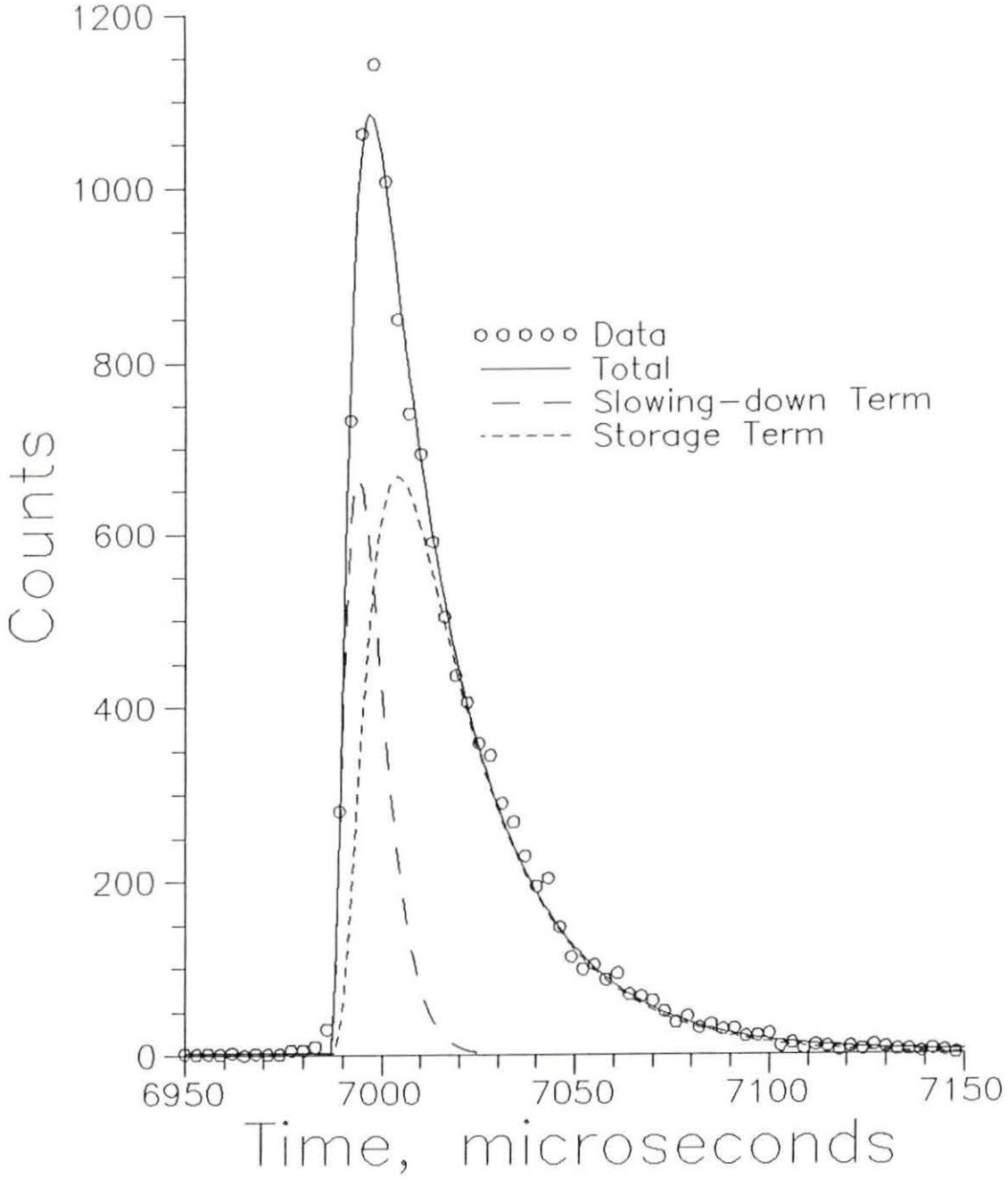

Figure 4.3: Ge(3,3,3) reflection for F moderator. The solid line is calculated by Equation 2.16

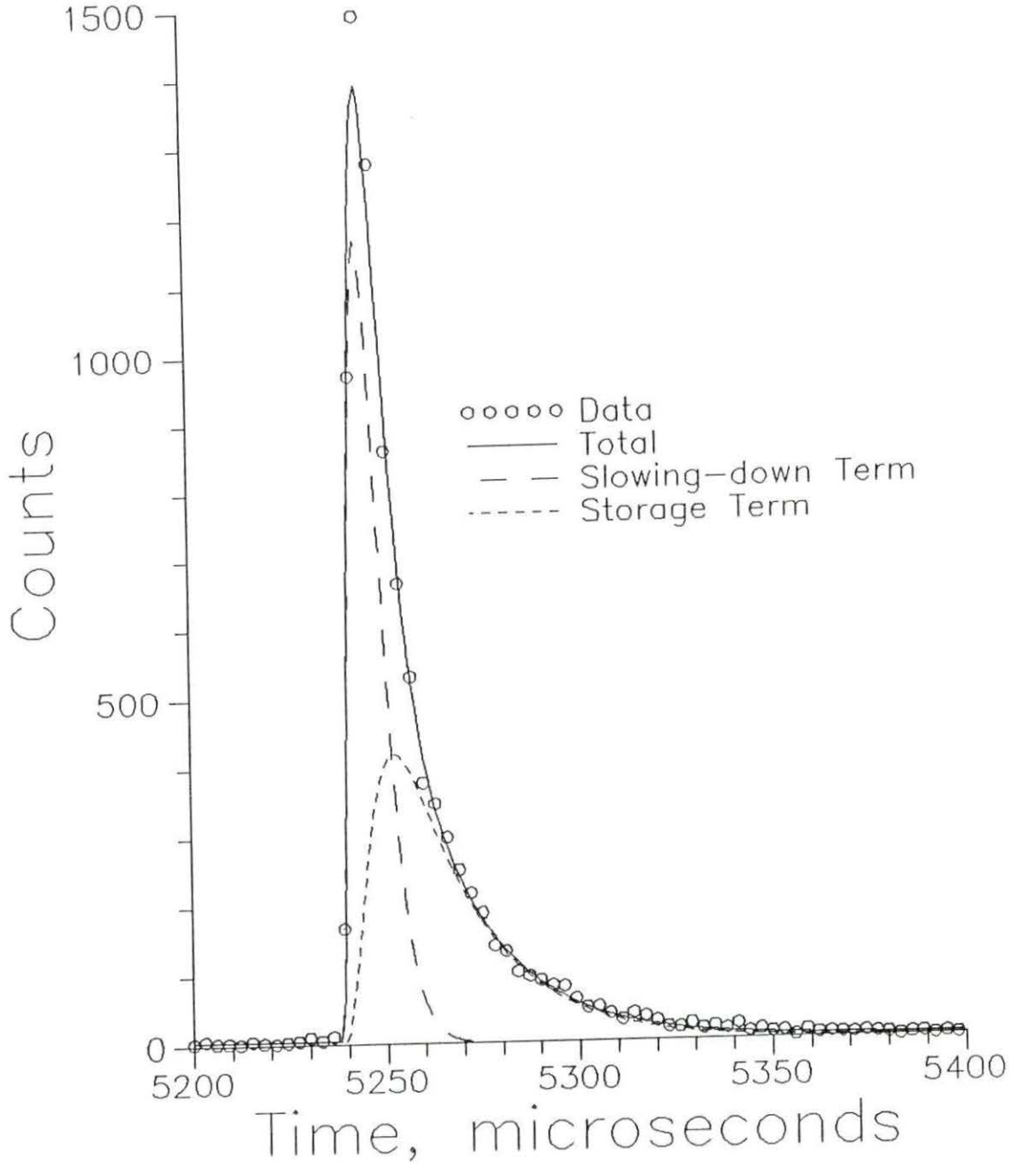

Figure 4.4: Ge(4,4,4) reflection for F moderator. The solid line is calculated by Equation 2.16

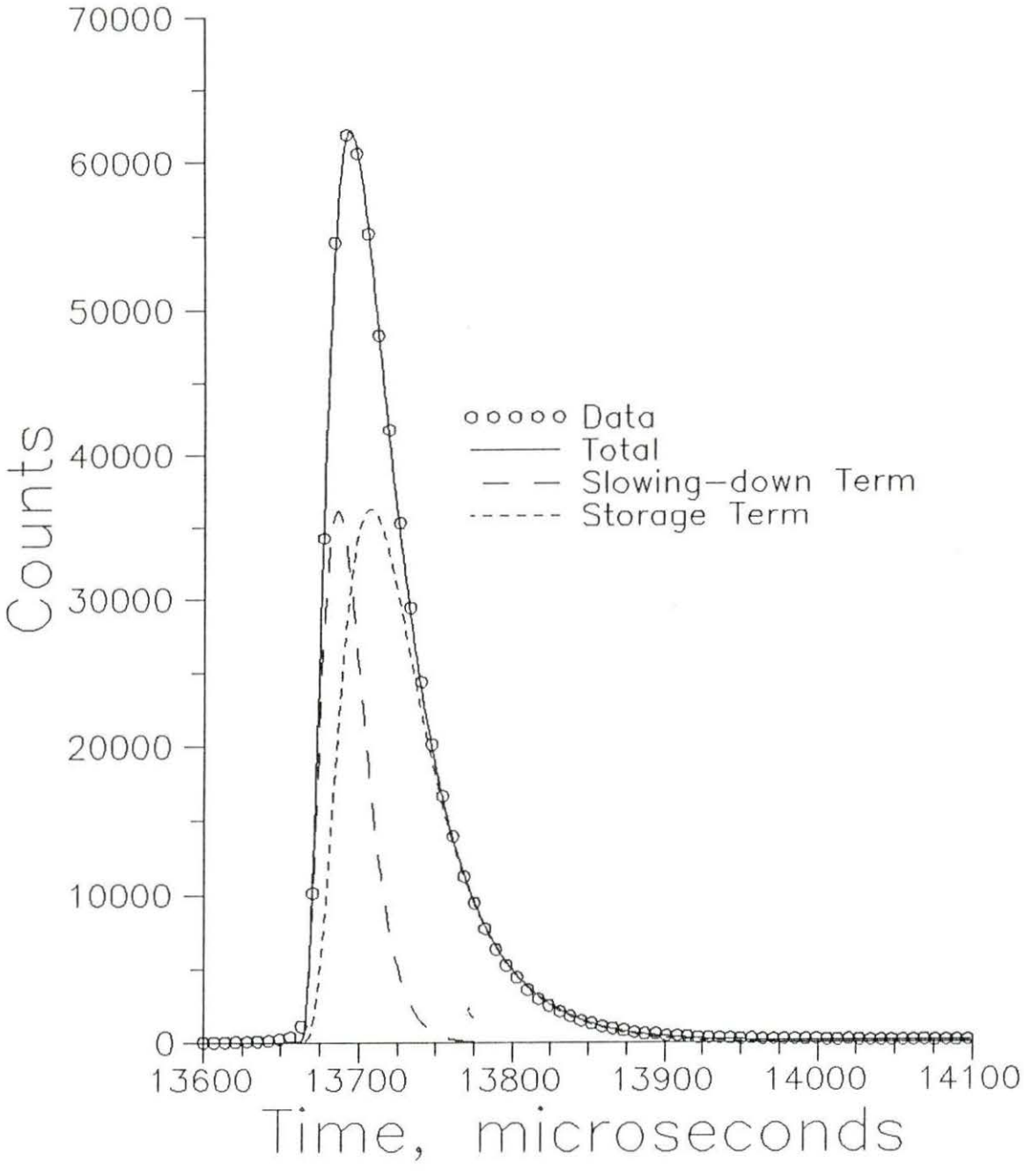

Figure 4.5: Ge(1,1,1) reflection for H moderator. The solid line is calculated by Equation 2.16

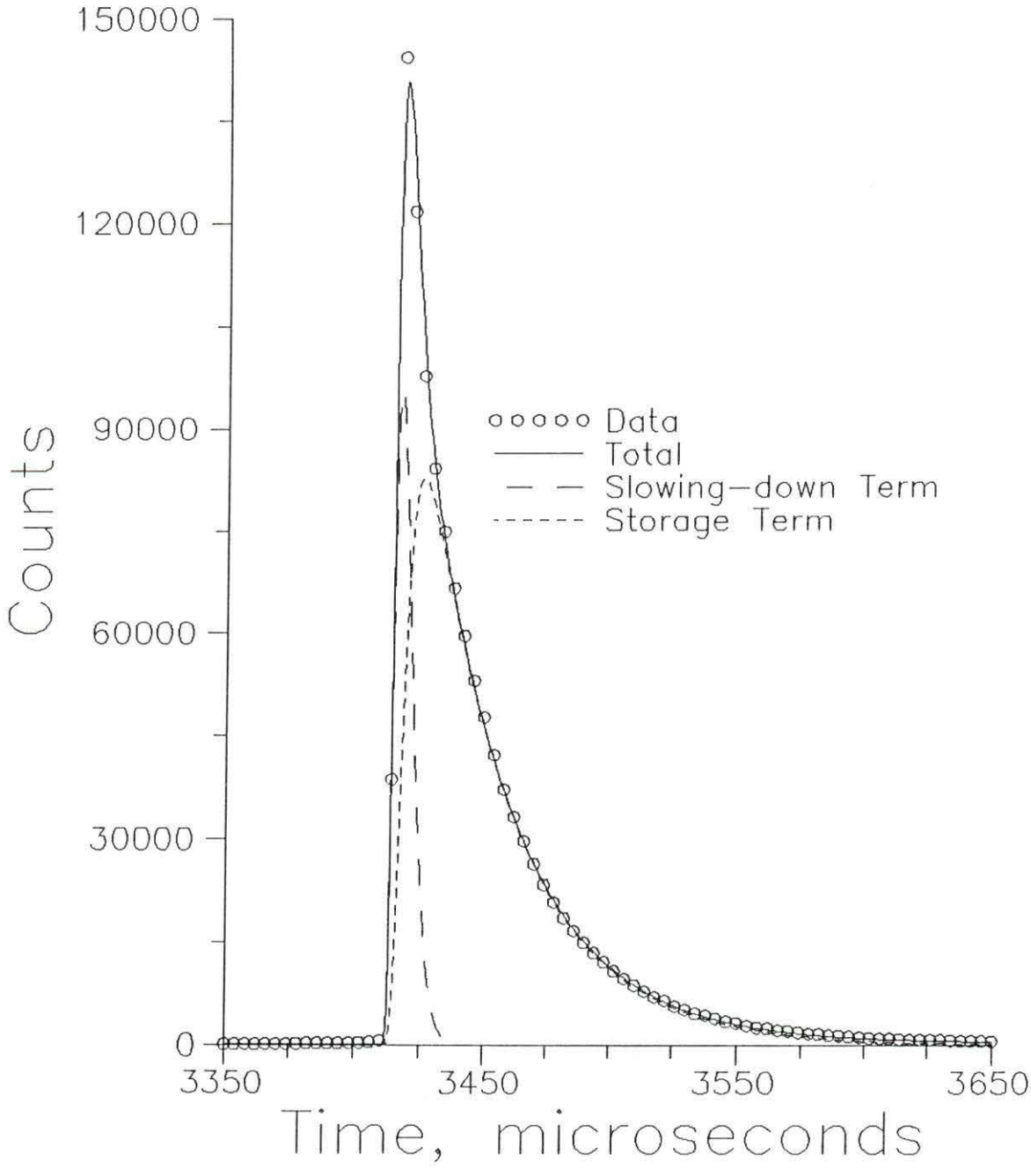

Figure 4.6: Ge(4,4,4) reflection for H moderator. The solid line is calculated by Equation 2.16

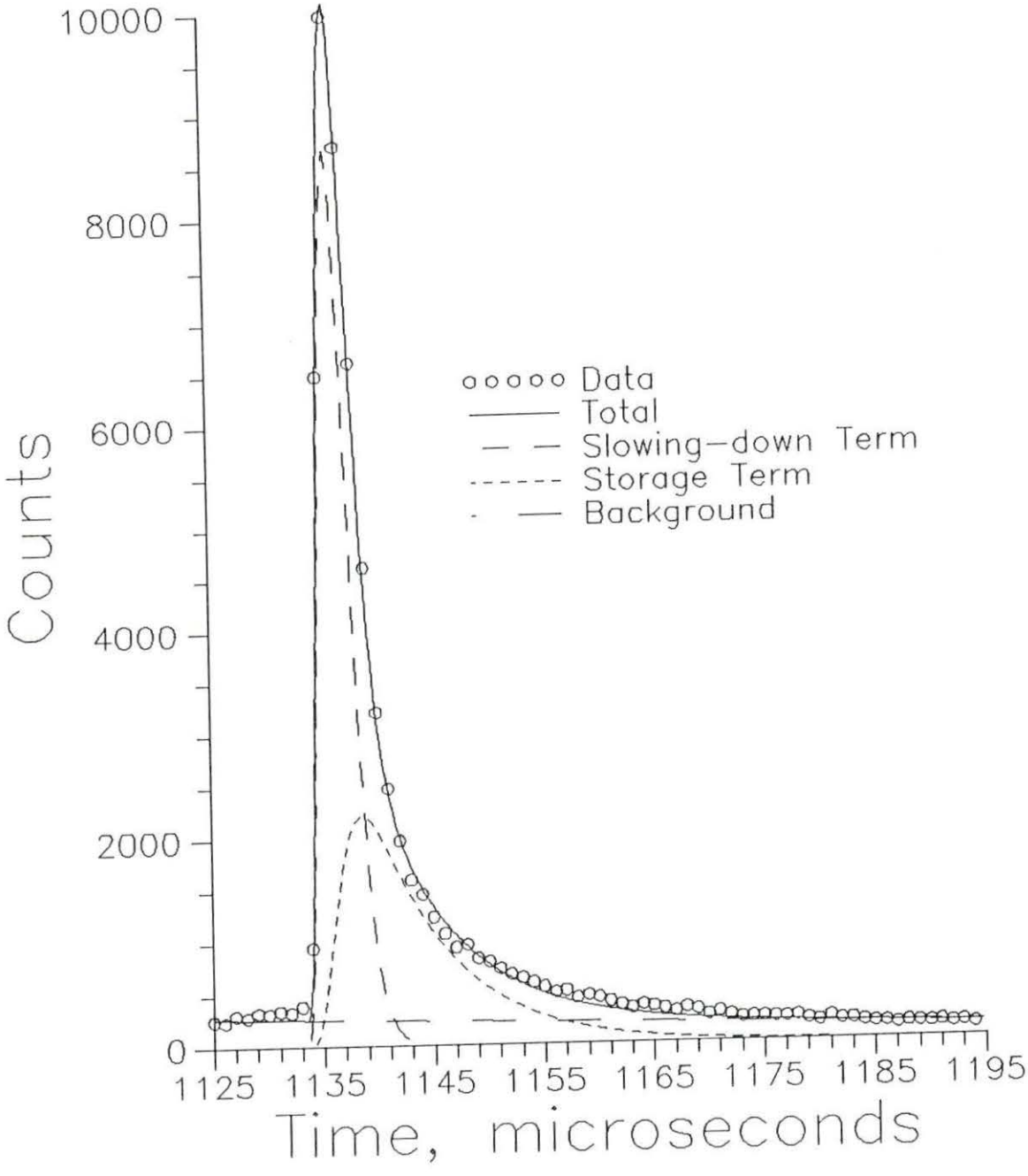

Figure 4.7: Ge(12,12,12) reflection for H moderator. The solid line is calculated by Equation 2.16

Table 4.2: Fitted parameters for the H moderator

n	t_0 (μs)	a (μs^{-1})	β (μs^{-1})	ν	R (%)	$Coef.\ of\ Det.$
1	13663	0.122	0.0263±0.0001	2.88±0.01	67.7 ±0.3	0.99761
3	4550.5	0.367	0.0233	2.68	92.6	0.98805
4	3411.6	0.489	0.0282	2.87	81.9	0.99632
5	2728.2	0.612	0.0509	3.53	53.4	0.98676
7	1947.2	0.857	0.0886	3.41	49.4	0.99426
8	1703.0	0.980	0.0887	3.62	45.9	0.99378
9	1513.3	1.10	0.110±0.0006	3.42±0.01	45.9±0.3	0.98987
11	1237.1	1.35	0.108	3.68	45.5	0.98810
12	1133.5	1.47	0.138	3.71	45.5	0.98052
13	1046.0	1.59	0.200	3.34	47.8	0.98393
15	905.83	1.84	0.129	3.27	51.8	0.97817
16	848.86	1.96	0.190	3.08	54.5	0.98247

The success of the generalized IC function in producing good fits to methane moderator pulse shape data unfortunately has not gone far in confirming any postulated wavelength dependence of parameters. Figures 4.8, 4.9, and 4.10 respectively show the fitted parameters β, R, and ν plotted as a function of wavelength. If the parameter β is expected to represent the fundamental decay constant of the moderator, it should be wavelength independent. At short wavelengths, the fitted parameter β is considerably larger than the value fitted at long wavelengths. Ikeda and Carpenter [17] observed the same phenomenon in polyethylene but not nearly to the same degree as in these measurements. They attributed the rise in β at short wavelengths to the diminished effect of the moderator decoupling material in this wavelength region. This introduces a tail on the pulse shape that decays faster than the storage term, but slower than the slowing-down term. This tail is principally taken up by the storage term in the least squares fitting process, therefore the decay constant of the storage term increases for short wavelengths above the expected constant value. Another explanation for an increased value of β at short wavelengths is the possibility of the existence of higher order exponentially-decaying transient terms.

The amplitude ratio parameter R is expected to have a value of nearly zero at short wavelengths, increasing to one at long wavelengths. This indicates the diminishing dominance of the slowing-down spectrum in representing the neutron pulse at longer wavelengths. Figure 4.9 shows this trend with the exception that the values of R at short wavelengths are larger than expected, an effect which is also attributed to the fitting of the pulse for short wavelengths.

The creation of the parameter ν was the goal of the generalization of the

original IC function. One postulated formulation of ν as a function of wavelength was presented as Equation 4.7. Figure 4.10 presents contrary evidence in that ν appears to be larger at short wavelengths, and to approach 2 at long wavelengths.

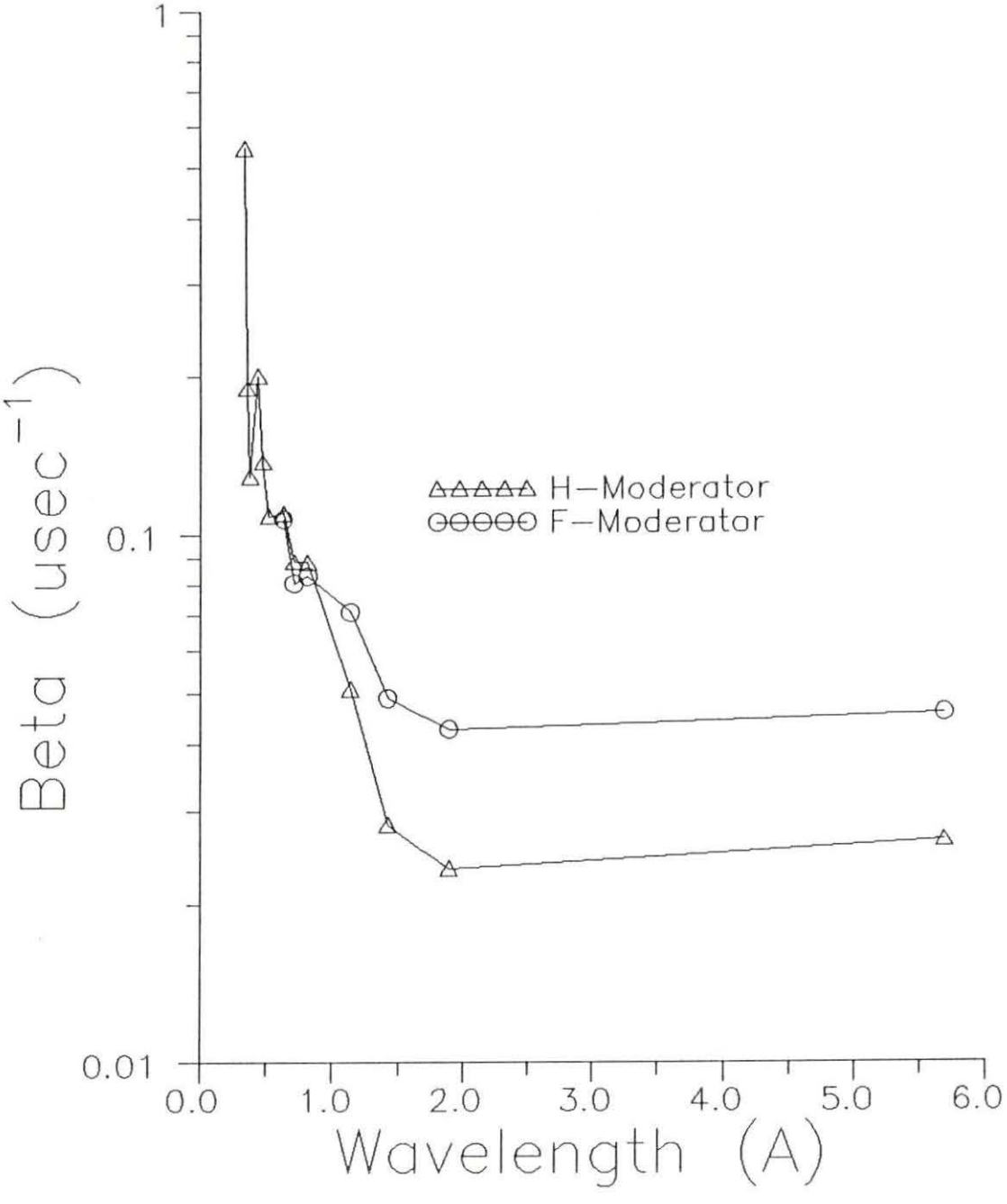

Figure 4.8: Wavelength dependence of β

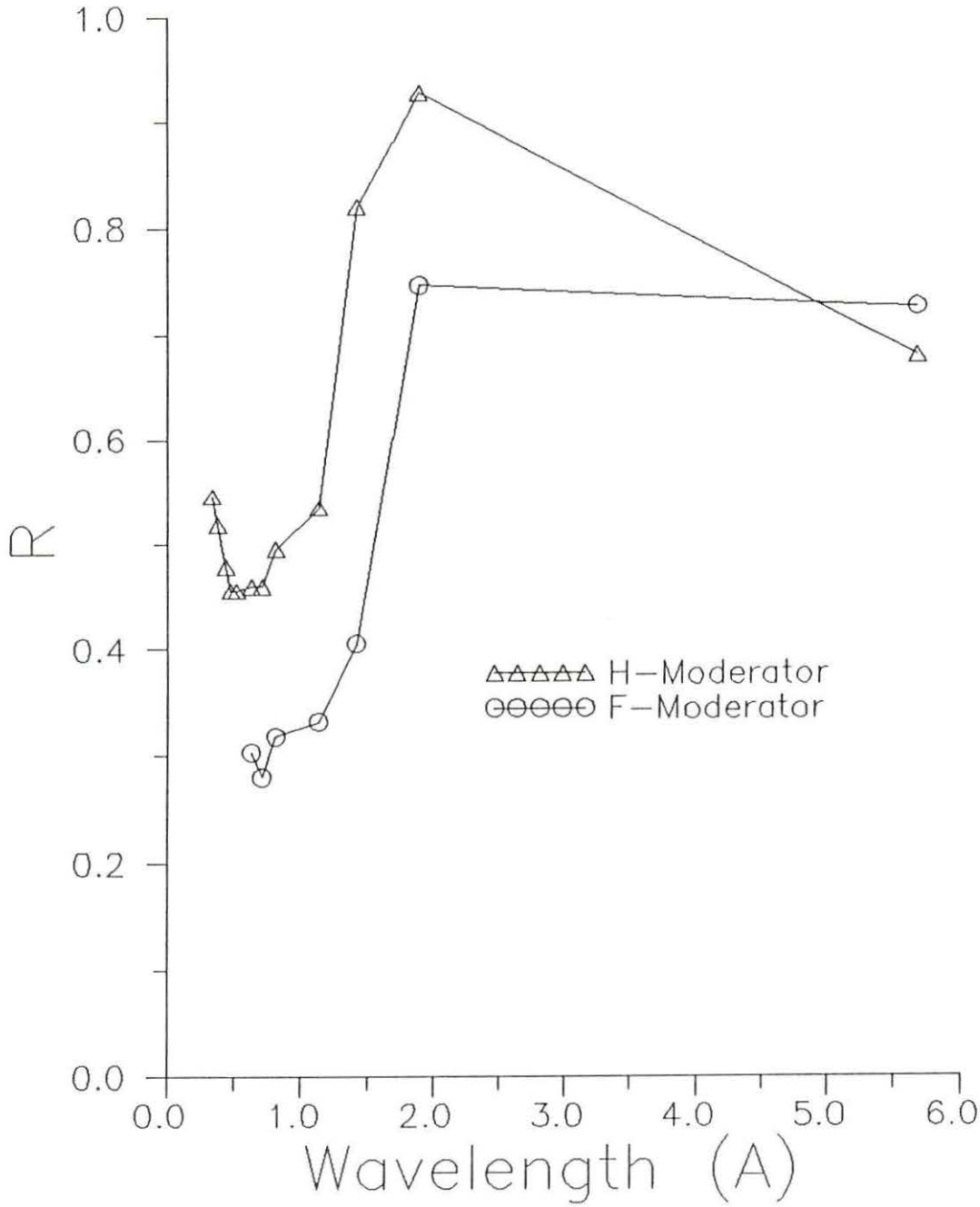

Figure 4.9: Wavelength dependence of R

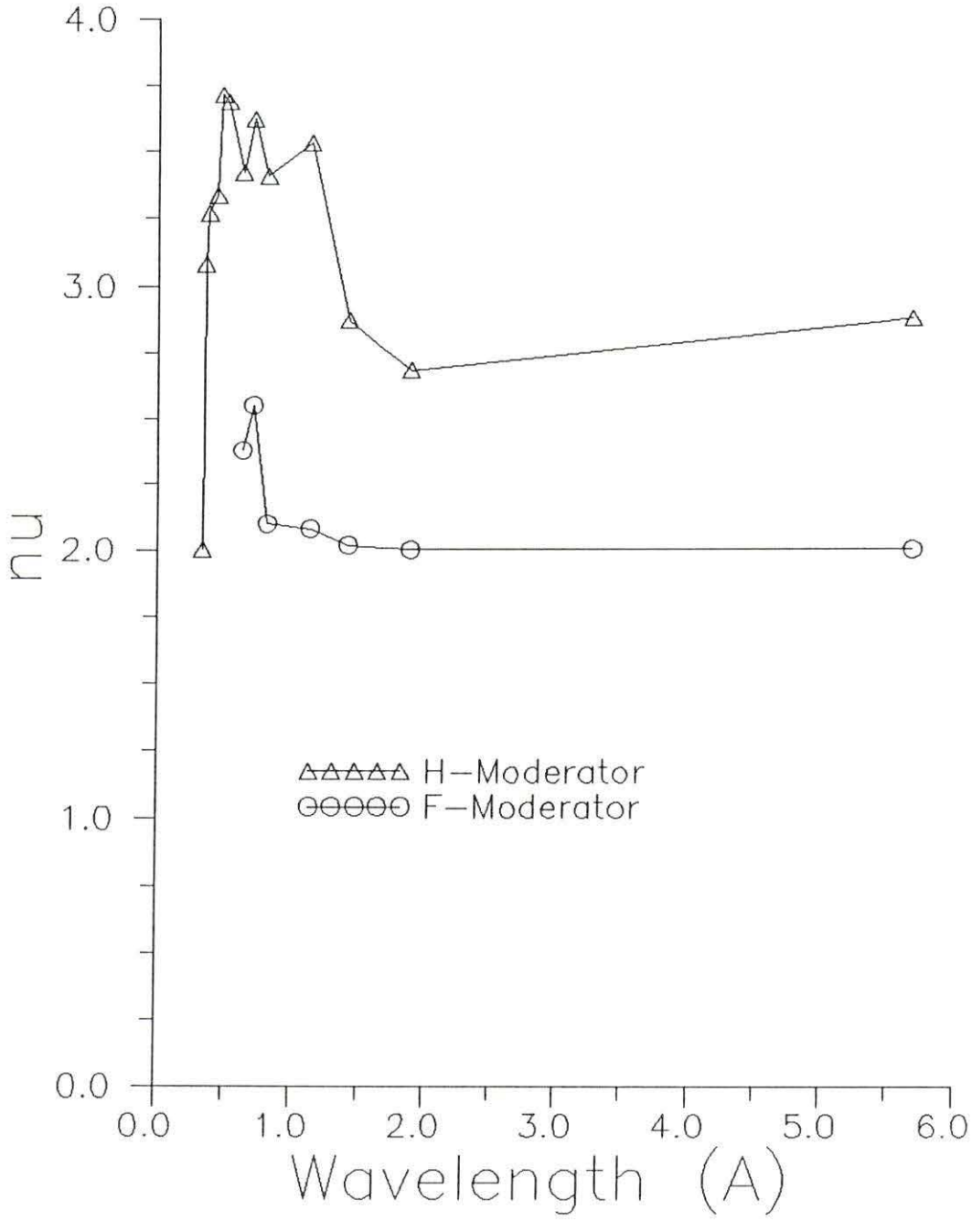

Figure 4.10: Wavelength dependence of ν

5 CONCLUSIONS AND SUGGESTIONS FOR FUTURE WORK

The purpose of this work was to measure the neutron emission-time distributions of the moderators at the Argonne National Laboratory Intense Pulsed Neutron Source. Fast neutrons entering the moderators following the source pulse are slowed down and emitted in broadened pulses. Mathematical functions are used to describe the shape of the pulses as a function of time and energy.

Measurements of the two liquid-methane and one solid-methane moderators were made by using a time-focused cooled-Ge crystal spectrometer and detector arrangement. Time focusing improves resolution of the observed pulses and cooling the monochromator crystal improves intensity at high neutron energies. Good data were collected from the liquid-methane F moderator through 200 meV and from the liquid-methane H moderator through 650 meV. Data were also collected from the solid-methane C moderator but no analysis has been attempted.

The Ikeda-Carpenter function was chosen to fit the measured data. This function was chosen because it has worked well in describing the shapes of neutron pulses from polyethylene moderators while providing a better physical description of pulse shapes than its predecessors. It contains two terms. The slowing-down term represents neutrons which emerge from the moderator in the process of slowing down before thermalization. The storage term represents neutrons which are

stored in the moderator and emerge after thermalization with a decay constant β. Analysis of the liquid-methane moderator data using non-linear least squares fitting techniques revealed substantial systematic deviations between the data and the best fitted function.

A generalization of the IC function was made to improve the quality of fits by replacing the exponent of the IC function slowing-down term with a wavelength-dependent parameter. The generalized IC function performed better at producing fits of the liquid-methane data. The coefficient of determination (R^2) for the fit of the first-order, 2.53 meV H moderator reflection was 0.9976.

Knowledge of the wavelength-dependence of the parameters in a pulse shape fitting function is necessary to provide precise information on the shapes of pulses over the entire range of wavelengths the moderator is used. The wavelength-dependence of the fitted parameters in the generalized IC function did not behave as expected. The decay constant β, expected to be independent of wavelength, was observed to increase by an order of magnitude at short wavelengths in the F and H moderator analyses.

The parameter R is the ratio of the area of the storage term component to the total area of a pulse shape. Its expected behavior is to approach a value of zero at short wavelengths and one at long wavelengths. The fitted parameter R in the F and H moderator analyses was observed to decrease as expected with decreasing wavelength but begin to increase at wavelengths less than 0.63 Å.

The parameter ν is the generalized exponent in the slowing-down term. Its observed behavior in the F and H moderator analyses was opposite of that expected, approaching a limit of 2 for long wavelengths instead of approaching 2 at short

wavelengths.

The above results indicate that additional research remains to be performed in this field. The following suggestions are made for future work:

(1) Additional measurements should be made of the liquid-methane moderators. Some changes in the pulse shapes may be expected due to the effects of the enriched uranium booster target.

(2) Geometrical alignment is very important in time focusing. Precision goniometers should be utilized to facilitate the measurement of angles and path lengths in the experimental arrangement.

(3) A variety of crystals should be used. A different crystal lattice spacing will provide an additional set of reflections. With more pulse shapes available in the wavelength continuum for analysis, wavelength dependence of fitting function parameters may be determined with greater confidence.

(4) Newly measured pulse shapes should be first analyzed with the original IC function. Wavelength dependence of parameters as well as quality of fits should be examined.

(5) If the original IC function again proves unsatisfactory, analysis should be tried with the generalized IC function. If the wavelength dependence of the parameters is still in question, further modification of the function may be necessary.

(6) Only after the liquid-methane moderator data have been adequately described by the fitting functions should analysis of the solid-methane moderator data be attempted. A functional form for these data will require components accounting for neutrons emerging from the tips of the fins and the bottoms of the grooves.

There remains a substantial amount of interest in the measurement of neutron

pulse shapes at IPNS. The installation of the booster target certainly will affect the pulse shapes of each moderator and the resolution of the time-of-flight instruments. Hopefully, the techniques developed in pulse shape measurement and analysis described in this thesis will serve as a foundation for further work in this area.

6 BIBLIOGRAPHY

[1] J. M. Carpenter, Nucl. Instr. Methods 145, 91 (1977).

[2] C. G. Windsor, *Pulsed Neutron Scattering* (Taylor and Francis Ltd., London, 1981).

[3] J. J. Duderstadt and L. J. Hamilton, *Nuclear Reactor Analysis* (John Wiley and Sons, Inc., New York, 1976).

[4] J. M. Carpenter and W. B. Yelon. "Neutron Sources." In *Methods of Experimental Physics: Neutron Scattering*, Vol. 23 part A. Eds. K. Sköld and D. L. Price. (Academic Press, Inc., Orlando, 1986). 157-196.

[5] D. E. Parks, M. S. Nelkin, J. R. Beyster, and N. F. Wikner, *Slow Neutron Scattering and Thermalization* (W. A. Benjamin, Inc., New York, 1970).

[6] A. E. Knox, J. M. Carpenter, J. L. Bailey, R. J. Armani, R. N. Blomquist, B. S. Brown, D. R. Henley, A. G. Hins, B. A. Loomis, A. W. Schulke, and H. R. Thresh, Proceedings of the 9th Meeting of the International Collaboration on Advanced Neutron Sources (ICANS-IX), Villigen, Switzerland, 1986, 557.

[7] J. M. Carpenter, Nucl. Instr. Methods 175, 287 (1980).

[8] F. J. Rotella, ed. Intense Pulsed Neutron Source Progress Report 1986-1988, Argonne National Laboratory, Argonne, 1988, 1-13.

[9] M. M. R. Williams, *The Slowing Down and Thermalization of Neutrons* (North-Holland Pub. Co., Amsterdam, 1966).

[10] J. H. Ferziger and P. F. Zweifel, *The Theory of Neutron Slowing Down in Nuclear Reactors* (The M. I. T. Press, Cambridge, Mass., 1966).

[11] J. R. Lamarsh, *Nuclear Reactor Theory* (Addison-Wesley Pub. Co., Reading, Mass., 1966).

[12] J. M. Carpenter, R. A. Robinson, A. D. Taylor, and D. J. Picton, Nucl. Instr. Methods A234, 542 (1985).

[13] D. F. R. Mildner, B. C. Roland, R. N. Sinclair, C. G. Windsor, L. J. Bunce, Nucl. Instr. Methods 152, 437 (1978).

[14] K. F. Graham and J. M. Carpenter, Nucl. Sci. Eng. 49, 418 (1972).

[15] J. M. Carpenter, M. H. Mueller, R. A. Beyerlein, T. G. Worlton, J. D. Jorgensen, T. O. Brun, K. Sköld, C. A. Pelizzari, S. W. Peterson, N. Watanabe, M. Kimura, and J. E. Gunning, Proc. Neutron Diffr. Conf., Petten, Netherlands, 1975, 192.

[16] F. Kropff, J. R. Granada, and R. E. Mayer, Nucl. Instr. Methods 198, 515 (1982).

[17] S. Ikeda and J. M. Carpenter, Nucl. Instr. and Methods A239, 536 (1985).

[18] C. G. Windsor and R. N. Sinclair, Acta Crystallogr. A32, 395 (1976).

[19] D. H. Day and R. N. Sinclair, Nucl. Instr. Methods 72, 237 (1969).

[20] I. Cole and C. G. Windsor, Nucl. Instr. Methods 171, 107 (1980).

[21] Personal communication with Dr. J. M. Carpenter, Argonne National Laboratory, September, 1987.

[22] R. G. Sachs and E. Teller, Phys. Rev. 60, 18 (1941).

[23] R. L. Bywater, Jr., R. E. Williams, and J. M. Carpenter, Proceedings of the 10th Meeting of the International Collaboration on Advanced Neutron Sources (ICANS-X), Los Alamos, 1988, in press.

[24] K. F. Graham and J. M. Carpenter, Nucl. Instr. Methods 85, 163 (1970).

[25] J. M. Carpenter, S. S. Cudrnak, C. M. DeCusatis, Proceedings of the 9th Meeting of the International Collaboration on Advanced Neutron Sources (ICANS-IX), Villigen, Switzerland, 1986, 315.

[26] P. R. Bevington, *Data Reduction and Error Analysis for the Physical Sciences* (McGraw-Hill Book Co., New York, 1969).

[27] J. J. Moré, B. S. Garbow, and K. E. Hillstrom, Argonne National Laboratory Report, ANL-80-74 (1980).

[28] C. P. Cox, *A Handbook of Introductory Statistical Methods* (John Wiley and Sons, Inc., New York, 1987).

7 ACKNOWLEDGEMENTS

I would like to express my thanks and warmest regards to Drs. Robert E. Williams and John M. Carpenter. Dr. Williams served as my major professor at Iowa State and has been a wonderful advisor and friend. Dr. Carpenter was my supervisor and mentor during my two summer appointments at Argonne National Laboratory. It was indeed a pleasure and privilege to work with him. I would also like to thank Dr. Herbert T. David and Mr. Peter Peterka of the ISU Statistics Department for their advice on curve fitting.

A special note of appreciation is extended to my wife, Shelly, for being my friend and tolerating my conversations on neutrons, moderators, pulse shapes, and things like that.

Portions of this work were funded by the U. S. Department of Energy through the Student Research Participation Program.